BBN SYSTEMS AND TECHNOLOGIES
A Division of Bolt Beranek and Newman Inc.

BBN Report No. 7943

Development of a High Target Strength Passive Acoustic Reflector for Low Frequency Sonar Applications

Final Technical Report

December 1993

Prepared by:

BBN Systems and Technologies
A Division of Bolt Beranek and Newman Inc.
10 Moulton Street
Cambridge, MA 02138

Sponsored by:

Defense Advanced Research Projects Agency
Undersea Warfare Office
AntiSubmarine Warfare Program
ARPA Order No. 7920
Issued by ONR under Contract N00014-91-C-0242
Transferred to DARPA Contract MDA972-91-C-0074

REPORT DOCUMENTATION PAGE

Form Approved
OMB No. 0704-0188

1. AGENCY USE ONLY (Leave blank)	2. REPORT DATE	3. REPORT TYPE AND DATES COVERED
	December 1993	Final Technical Report, Sept. 1991–Oct. 1993

4. TITLE AND SUBTITLE
Development of a High Target Strength Passive Acoustic Reflector for Low Frequency Sonar Applications

5. FUNDING NUMBERS
ARPA Order No. 7920
ONR Contract
N00014-91-C-0242
DARPA Contract
MDA972-91-C-0074

6. AUTHOR(S)
Charles Malme, Paul Jameson, Paul McElroy,
David Stracher, Gary Thomas, Daniel Zwillinger

7. PERFORMING ORGANIZATION NAME(S) AND ADDRESS(ES)
BBN Systems and Technologies
A Division of Bolt Beranek and Newman Inc.
10 Moulton Street
Cambridge, MA 02138

8. PERFORMING ORGANIZATION REPORT NUMBER
7943

9. SPONSORING/MONITORING AGENCY NAME(S) AND ADDRESS(ES)
Defense Advanced Research Projects Agency
Undersea Warfare Office
Antisubmarine Warfare Program
3701 North Fairfax Drive
Arlington, VA 22203-1714

10. SPONSORING/MONITORING AGENCY REPORT NUMBER
None

11. SUPPLEMENTARY NOTES

12a. DISTRIBUTION/AVAILABILITY STATEMENT

12b. DISTRIBUTION CODE

13. ABSTRACT (Maximum 200 words)

Our objective was development of a broadband passive acoustic reflector with a high target strength to serve as a low-cost target for low frequency sonar trials and fleet exercises. The primary development goals included calibrated, stable monostatic and bistatic reflectivity and adjustable deployment depth down to 90 m. The development used both computer models and 1/4-scale physical models. Resonant air-filled cylinders were found to provide the highest TS values for a given reflector volume, the resonance occurring at ka = 0.02 at the depth of interest. Their target strength at resonance approximates that at ka = 1.0 with a variation of only ±4 dB between, yielding a broad operating range. A prototype reflector was assembled using a 16-m length of gum-rubber tubing (3.2 cm ID). Tubing inflation was maintained by a SCUBA regulator. Test results at a depth of 90 m showed an effective target strength of 12 dB at 250 Hz, varying within ±2 dB from 200 to 400 Hz. Subsequently, a 32-m unit was designed, built, and utilized in a sea test. This unit has enhanced bandwidth to a lower frequency of 100 Hz, achieved with four tubing sizes ranging from 3.2 to 7.6 cm ID.

14. SUBJECT TERMS
Passive reflector, cylindrical reflector, target, high target strength, low frequency, LFA, low cost, calibrated, stable, monostatic target strength, bistatic target strength, air-filled, rubber tube

15. NUMBER OF PAGES
50 plus iii

16. PRICE CODE

17. SECURITY CLASSIFICATION OF REPORT	18. SECURITY CLASSIFICATION OF THIS PAGE	19. SECURITY CLASSIFICATION OF ABSTRACT	20. LIMITATION OF ABSTRACT
Unclassified	Unclassified	Unclassified	

BBN Report No. 7943

Development of a High Target Strength Passive Acoustic Reflector for Low Frequency Sonar Applications

Final Technical Report

December 1993

C. I. Malme
P. Jameson
P. McElroy
D. Stracher
G. Thomas
D. Zwillinger

Prepared by:

BBN Systems and Technologies
A Division of Bolt Beranek and Newman Inc.
10 Moulton Street
Cambridge, MA 02138

Sponsored by:

Defense Advanced Research Projects Agency
Undersea Warfare Office
AntiSubmarine Warfare Program
ARPA Order No. 7920
Issued by ONR under Contract N00014-91-C-0242
Transferred to DARPA Contract MDA972-91-C-0074

CONTENTS

LIST OF FIGURES

LIST OF TABLES

DEVELOPMENT OF A HIGH TARGET STRENGTH PASSIVE ACOUSTIC REFLECTOR FOR LOW FREQUENCY SONAR APPLICATIONS

ABSTRACT

The objective of this study was development of a broadband passive acoustic reflector with a high target strength to serve as a convenient, low-cost target for low frequency sonar trials and fleet exercises. The primary development goals included calibrated, stable monostatic and bistatic reflectivity and adjustable deployment depth down to 90 m (300 ft). The development process used both computer models and 1/4-scale physical models to determine the most effective configuration capable of meeting the project goals. Review of acoustic scattering theory showed that, for similarly-sized objects, acoustically-soft reflectors (bubbly liquids or air-filled spheres and cylinders) are capable of providing higher target strength values than hard reflectors (metal spheres or corner-reflectors). Air-filled cylinders were found to provide the highest target strength values for a given reflector volume. This is a result of the tube resonance frequency occurring at ka=0.02 at the depth range of interest, where k is the acoustic wavenumber and a is the tube radius. Air-filled cylinder target strength at resonance is about equal to its target strength at ka=1.0 with a variation of only about ±4 dB between these values. This enables an air-filled cylinder to have enhanced reflectivity over a much broader operating range than an air-filled sphere that has enhanced reflectivity only near the resonance frequency. Guided by study results, a prototype reflector was assembled using a 16-m length of air-filled gum rubber tubing, 5.7 cm in diameter (3.2 cm ID). Tubing inflation was maintained by a SCUBA regulator attached to a small air tank. Test results at a depth of 90 m showed an effective target strength of 12 dB at 250 Hz with a variation within ±2 dB from 200 to 400 Hz. This is equivalent to the target strength of a 16-m diameter sphere—an object with a volume about 52,000 times that of the prototype cylinder reflector. Subsequently, a 32-m unit was designed, built, and utilized in a sea test. This unit has enhanced bandwidth to a lower frequency of 100 Hz, achieved with four tubing sizes ranging from 3.2 to 7.6 cm ID.

ACKNOWLEDGMENTS

This work was supported by the Advanced Research Projects Agency under Contract No. MDA972-91-C-0074. The senior author extends special thanks to Mary Lou Frey who adapted Stanton's analysis for use on personal computers, Paul Jameson and Dan Zwillinger for ARMAC

Model and near-field correction analysis, Gary Thomas for design assistance and fabrication of the reflector, and David Stracher for assistance with the model tests.

1. SUMMARY

The results of the study have shown that low-cost, conveniently deployed, high target strength reflectors can be fabricated using gas-filled compliant tubing. Near the fundamental resonant frequency of the tubing, the target strength is directly proportional to the length of the tubing and independent of tube diameter. For a given tube diameter, at normal incidence to the tube axis, theory shows that the target strength will vary less than ±4 dB for $.004 \leq ka \leq 1$. In the plane of the tube axis the beampattern of the backscattered energy becomes narrower with increasing frequency. This places a practical limit on the upper frequency range of a given design that depends on the maintenance of tube alignment and on the coherence of the incident sound signal over the length of the reflector.

2. INTRODUCTION

The purpose of the study was to investigate the feasibility of developing efficient, easily-deployed, high target strength[1] passive acoustic reflectors for use in low frequency active sonar trials and general fleet exercises. The project goal was to obtain a high target strength over a broad frequency range, reaching a level of 15 dB at 250 Hz. The design was to provide stable reflective properties that could be easily calibrated. An omnidirectional horizontal reflectivity was desirable for bistatic applications. The vertical reflectivity could be optimized for horizontal sound incidence, since steep sound arrival angle operation was not anticipated. The operating depth was to be at least 90 m (300 ft). Size and weight of the unit before deployment were important design considerations to simplify storage and handling.

3. METHODS

The methods used in the study incorporated both theoretical analysis and experimental testing to optimize reflector design parameters. The initial experimental testing was performed with 1/4 and

[1] Target Strength (TS) as defined by Urick (1983) is $10\text{Log}_{10}(I_r/I_i)$ where I_r is the reflected sound intensity at 1 m from the center of a target and I_i is the incident intensity from a distant source.

1/10 scale models in a water tank test facility. Subsequent full scale testing was done in a flooded quarry facility and at the U.S. Naval Underwater Weapons Center (NUWC) Seneca Lake Facility. Size limitation of the model test tank required the use of a pulsed source and a time-gated receiver to minimize reverberation interference with the target echo. A computer-controlled measurement system, shown in Fig. 1A, was assembled to control the test procedure and provide the capability of using coherent cancellation techniques to minimize first-order boundary reflection interference. The test arrangement shown in Fig. 1B provided the capability of obtaining both monostatic and bistatic target strength data.

Test signals typically consisted of short tone bursts of about 3 msec duration. Usually at least 3 test replications were made at any given frequency and the recorded echo signals averaged to reduce the influence of background noise. The test procedure involved several steps. The tank echo pattern was recorded for the reference condition with no target present. The target was then placed in position and the test repeated. The averaged echo signal for the reference condition was then subtracted from the averaged echo signal for the target present condition, using the same time delay reference. This process greatly reduced the level of the transmitted and first order reflected signals so that the echo signal level could be measured for conditions of direct and echo signal overlap. Figure 2 shows an example of this process. The target strength of a given reflector was determined by calculating the average acoustic intensity within a selected time window (usually 2 msec) for both the incident and echo pulses and then applying the appropriate sonar equation for the test geometry. This procedure was computer-implemented in real time so that target strength data were immediately available to facilitate the testing process.

3.1 Comparison of Design Alternatives

Several well known acoustic scattering principles were considered and evaluated during the study for potential application to the reflector design problem. While rigid spheres and cylinders as well as corner reflectors have useful broadband scattering characteristics, they were considered impractical because of the large physical sizes required in the low frequency operating range. Consequently, after a review of alternatives, the initial study effort was directed at testing the promising concept of fluid reflectors. High reflectivity was theoretically achievable from a fluid volume with a sound speed appreciably lower than that of the surrounding water. The low sound speed was to be produced and controlled by creating or injecting clouds of small bubbles into a contained volume of water to provide the correct gas volume fraction. Work on this idea led to the development of a pump-driven recirculating bubble reflector and then to a test design using several

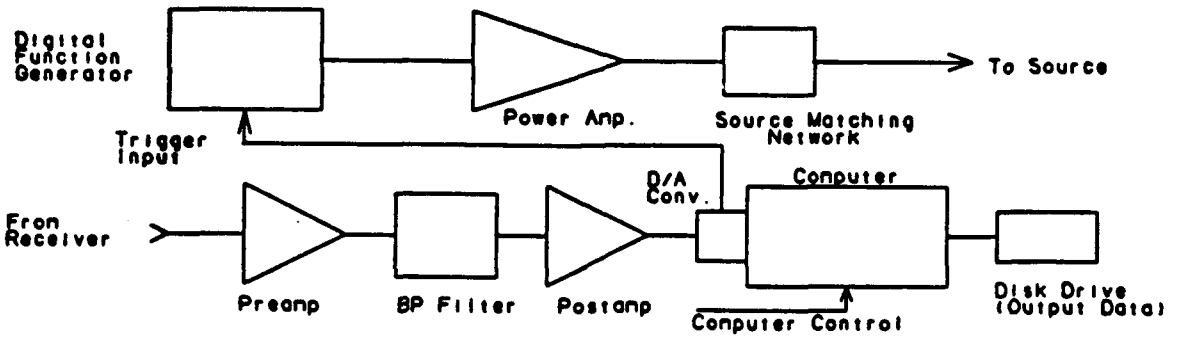

A. Block diagram of test instrumentation.

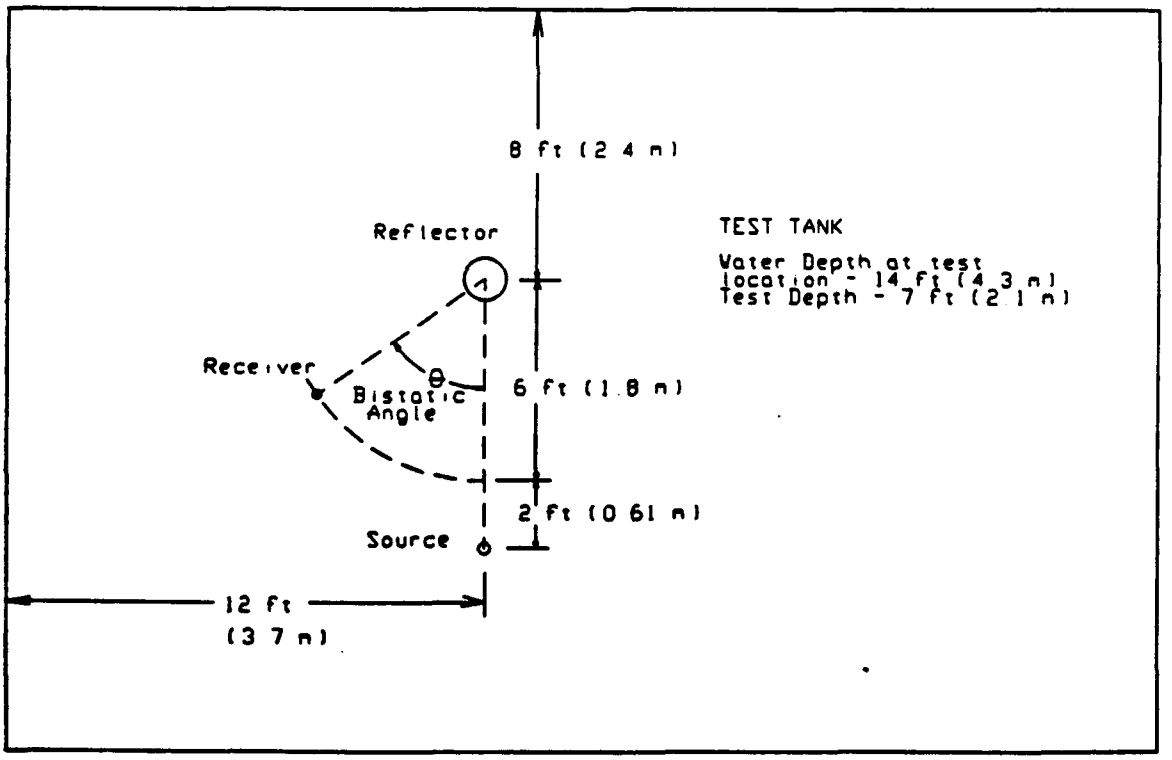

B. Test geometry for target strength measurements.

Figure 1. Arrangement for scale-model tank testing.

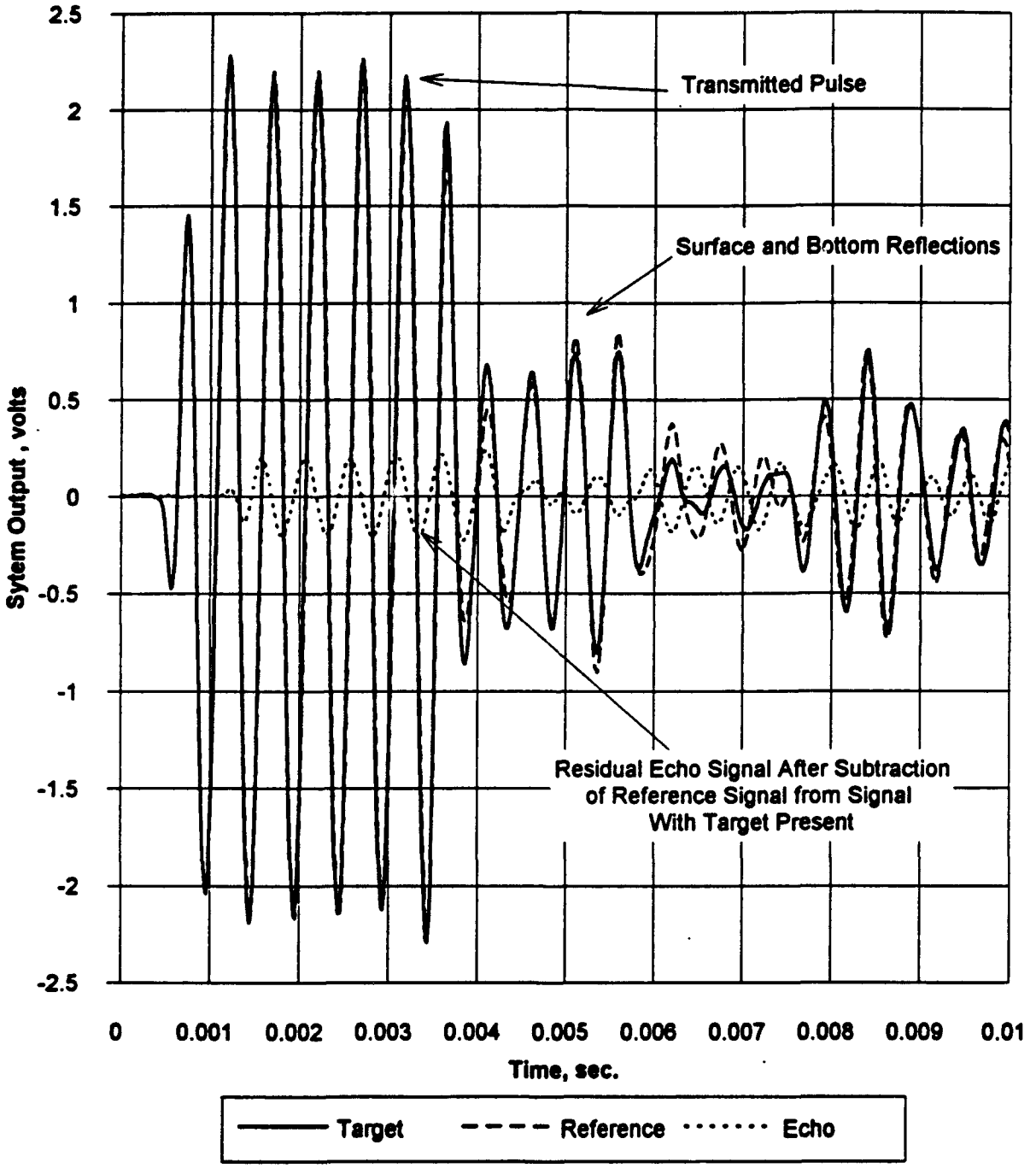

Figure 2. Example of pulse-echo processing to reduce direct pulse and first-order reflection interference.

air-filled compliant tubes to simulate a stable bubble distribution. The reflectivity of this tube-filled volume was found to be comparable to that of an air-filled cylinder of the same dimensions. This, in turn, led to the selection of a single, long, air-filled tube as the prototype reflector technology that provided the best match to the required design features. The following discussion describes the evolution of the study.

3.1.1 The Bubble Cloud Reflector

The theory guiding this work has been developed by Anderson (1950), Carey et al. (1990), and others. They have shown that if a bubble cloud is created with small bubbles having resonant frequencies higher than the desired range of reflector operation, then the resulting sound speed in the bubble cloud is lower than that of the surrounding water. Furthermore, if the gas-volume fraction is adjusted properly, the bubbly water volume exhibits a reflectivity much higher than that of a rigid sphere of the same dimensions. Figure 3, from Anderson (1950), shows the predicted reflectivity for direct backward scattering from fluid spheres of dimensions comparable to a wavelength. Reflectivity is shown as a function of sound speed ratio[2] h and normalized circumference[3] ka for a density ratio g of 1. The figure shows that for low sound speed fluids (h<1) the reflectivity is increased significantly.

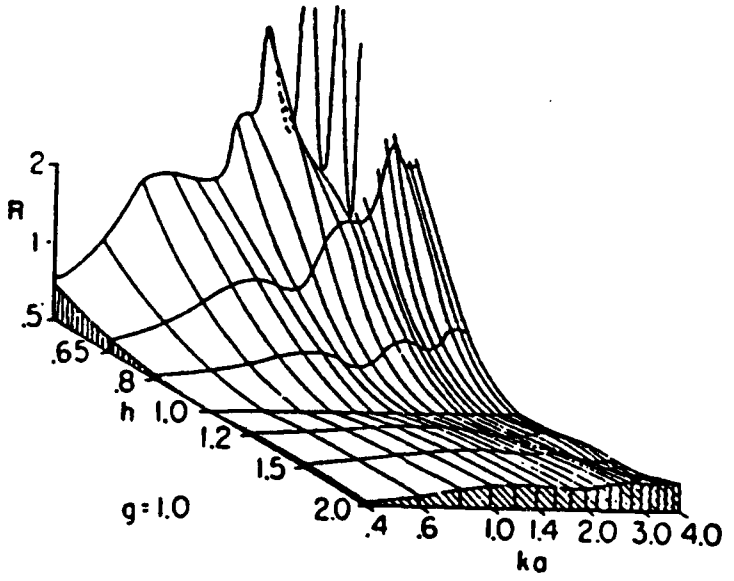

Figure 3. Reflectivity R for direct backward scattering from fluid spheres of dimensions comparable to a wavelength (from Anderson 1950).

[2] The sound speed ratio *h* is defined as the ratio of the sound speed inside the reflector to the sound speed in the outside fluid. Similarly, the density ratio *g* is defined as the ratio of the density of the fluid inside the reflector to the density of the outside fluid.

[3] To aid analysis, the dimensions of a scattering object are often normalized by the acoustic wavelength. For spheres and cylinders, the circumference ($2\pi a$) is divided by the wavelength (λ). Since the acoustic wavenumber, $k = 2\pi/\lambda$, this results in the normalized dimension, ka.

A test reflector assembly using a confined cylindrical volume of free bubbles was fabricated inside a thin vinyl tube, as shown in Fig. 4A. This design was intended to provide a means of injecting small gas bubbles into a known volume of water while concurrently preventing larger bubbles of gas from escaping into the surrounding medium due to buoyancy and turbulence forces. This was achieved by combining a submersible pump with an aspirator pump to continually recirculate air from the initial preset volume at the top of the assembly through the pump and manifold thereby regenerating bubbles of a defined size. A photo of the completed assembly is shown in Fig. 4B.

The required bubble radius was found from the bubble resonance equation (adapted from Urick 1983)

$$a = (316/f_0)(1+0.1Z)^{.5} \quad \text{(cm)} \qquad (1)$$

where f_0 is the resonance frequency (Hz) and Z is depth (m). For the 1/10 scale reflector shown in Fig. 4A, the bubble radii were required to be smaller than about 1 mm, corresponding to a resonance frequency of 3.6 kHz under the test conditions used.

The bubble recirculation process tended to reduce the number of large bubbles that rose more rapidly through the target volume than smaller bubbles of the desired size so that a stable distribution was eventually achieved. The interior volume of the target became filled with the desired cloud of small bubbles as shown in the photo of Fig. 5, but unfortunately many bubbles also adhered to the plastic film envelope of the reflector assembly. These bubbles became effectively a continuous air layer. This likely reduced the sound intensity reaching the interior of the bubble cloud to produce the multiple reflections required to achieve target strength values predicted by theory.

As shown in the target strength data of Fig. 6, values up to -9 dB were observed at 2 kHz for a short interval when a good bubble distribution was obtained in the enclosed volume. However, when the envelope became covered with bubbles, the target strength was reduced to -12 dB. This value is approximately equal to the target strength predicted for a gas-filled cylinder 0.2 m (8 in.) in diameter, 0.8 m (32 in.) long (the dimensions of the reflector envelope). If the optimum bubble distribution had been achieved with multiple reflections from the interior volume, a target strength of -2 dB was predicted.

In an attempt to prevent bubble coalescense on the target wall, the water-bubble mixture distribution system was redesigned to incorporate a rotating mechanical sprinkler head as shown in

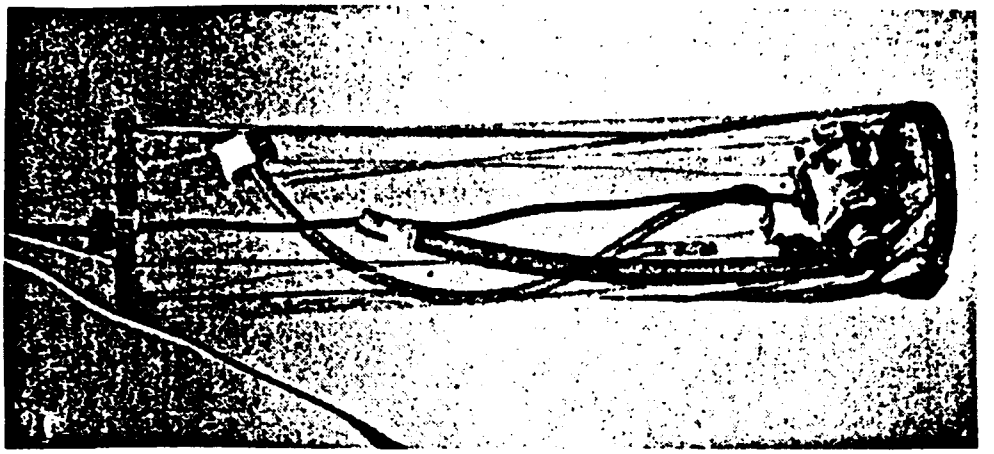

B. Photo of bubble target assembly prior to deployment

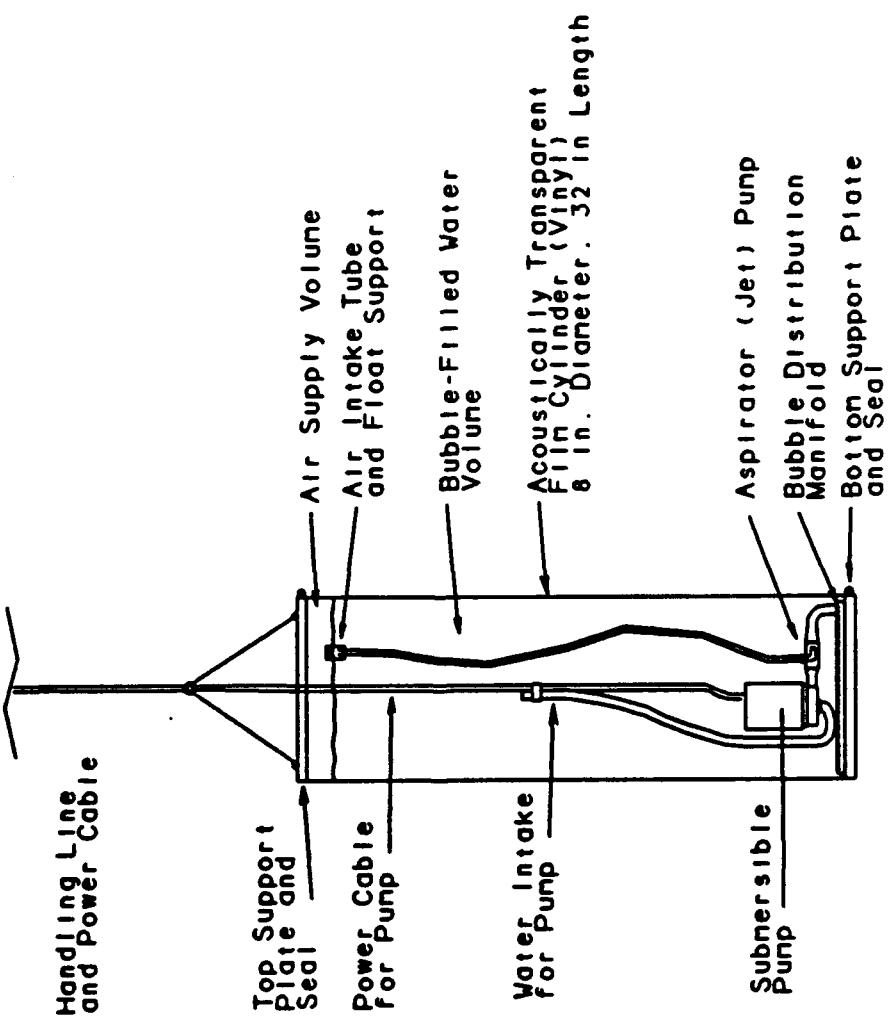

A. Component arrangement.

Figure 4. Bubble recycling target.

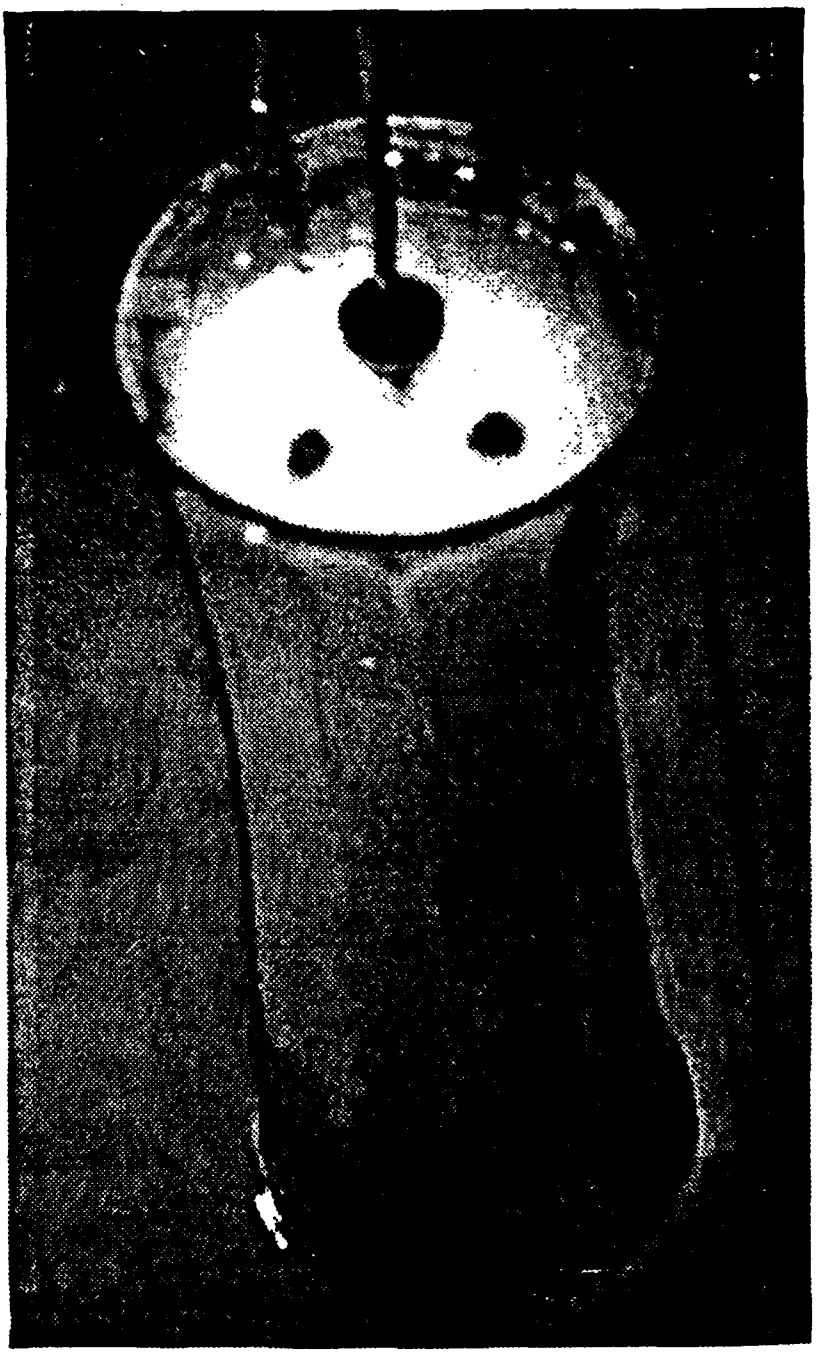

Figure 5. Photo of deployed bubble target.

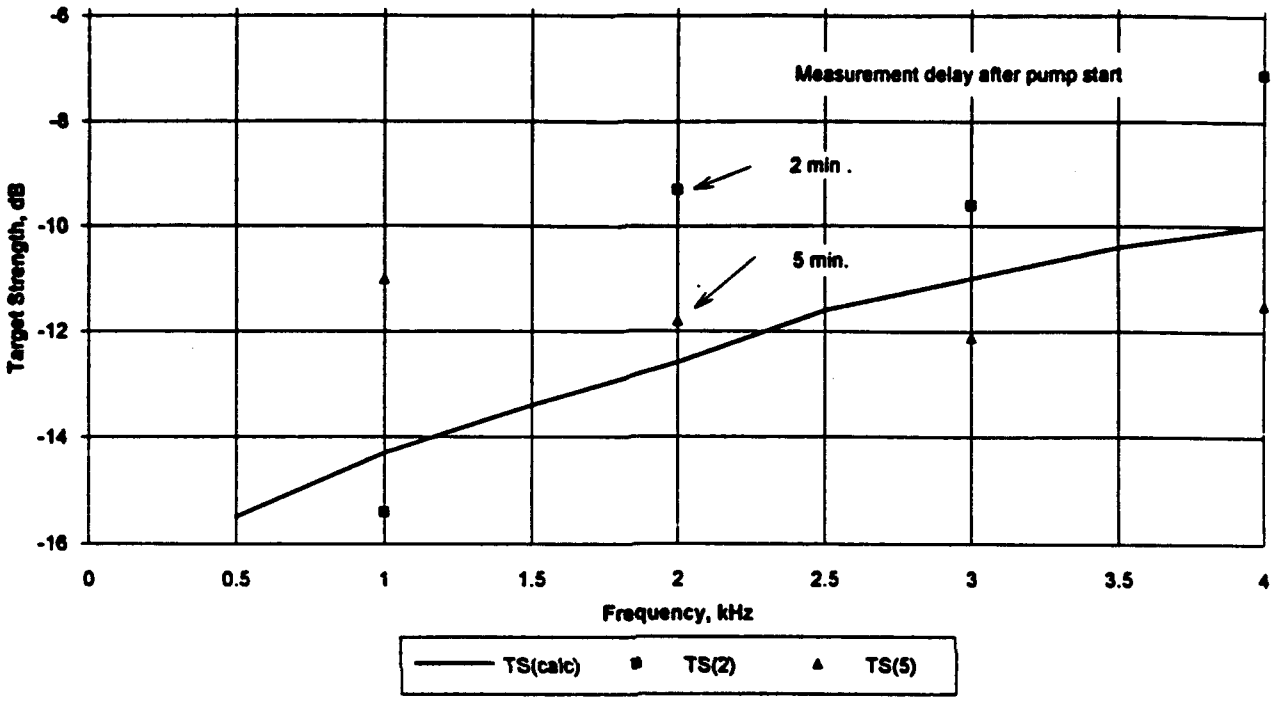

Figure 6. Bubble recycling target strength data. Backscatter target strength compared with calculated values for air-filled cylinder, a=0.104 m, L=0.81 m.

Fig. 7. It was hoped that the velocity of the ejected fluid would sweep the bubbles off the vinyl film wall. This did actually occur, but only near the sprinker head. As a result, no long-term increase in the target strength was observed.

3.1.2 Multiple Tube Reflector

Because of the difficulty in obtaining a low sound speed fluid reflector by producing the correct bubble size and volume distribution in a stable test configuration, we sought to simulate a bubble-filled volume by using a matrix of air-filled compliant tubing. Reflectors were constructed using a cylindrical volume filled with many small-diameter gum-rubber tubes. Gum rubber was selected because of its relatively low dynamic modulus of elasticity. We did not want to greatly increase the effective stiffness of the air column in the tubes. A typical reflector configuration, shown in Fig. 8, consisted of a cylindrical arrangement of vertical tubes, held between two plastic support plates.

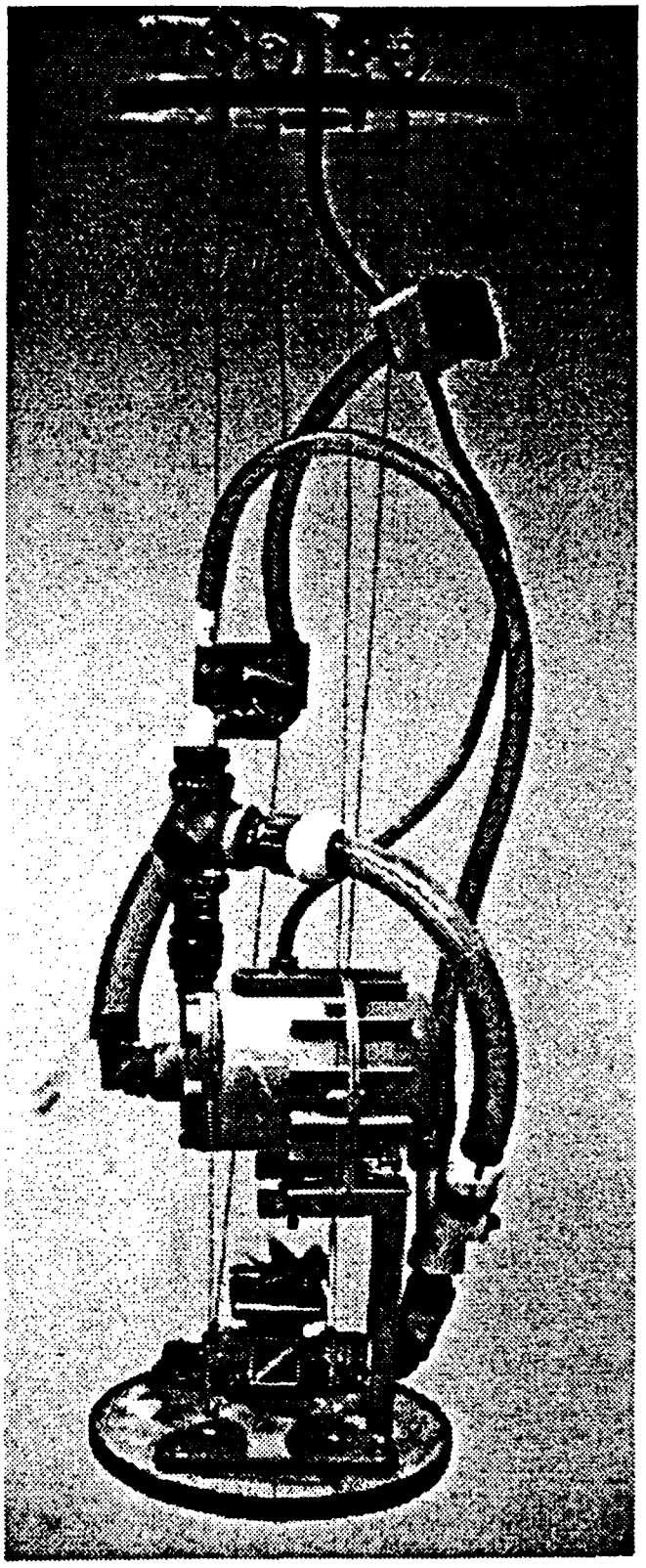

Figure 7. Photo of bubble recycling target with mechanical flow augmentation.

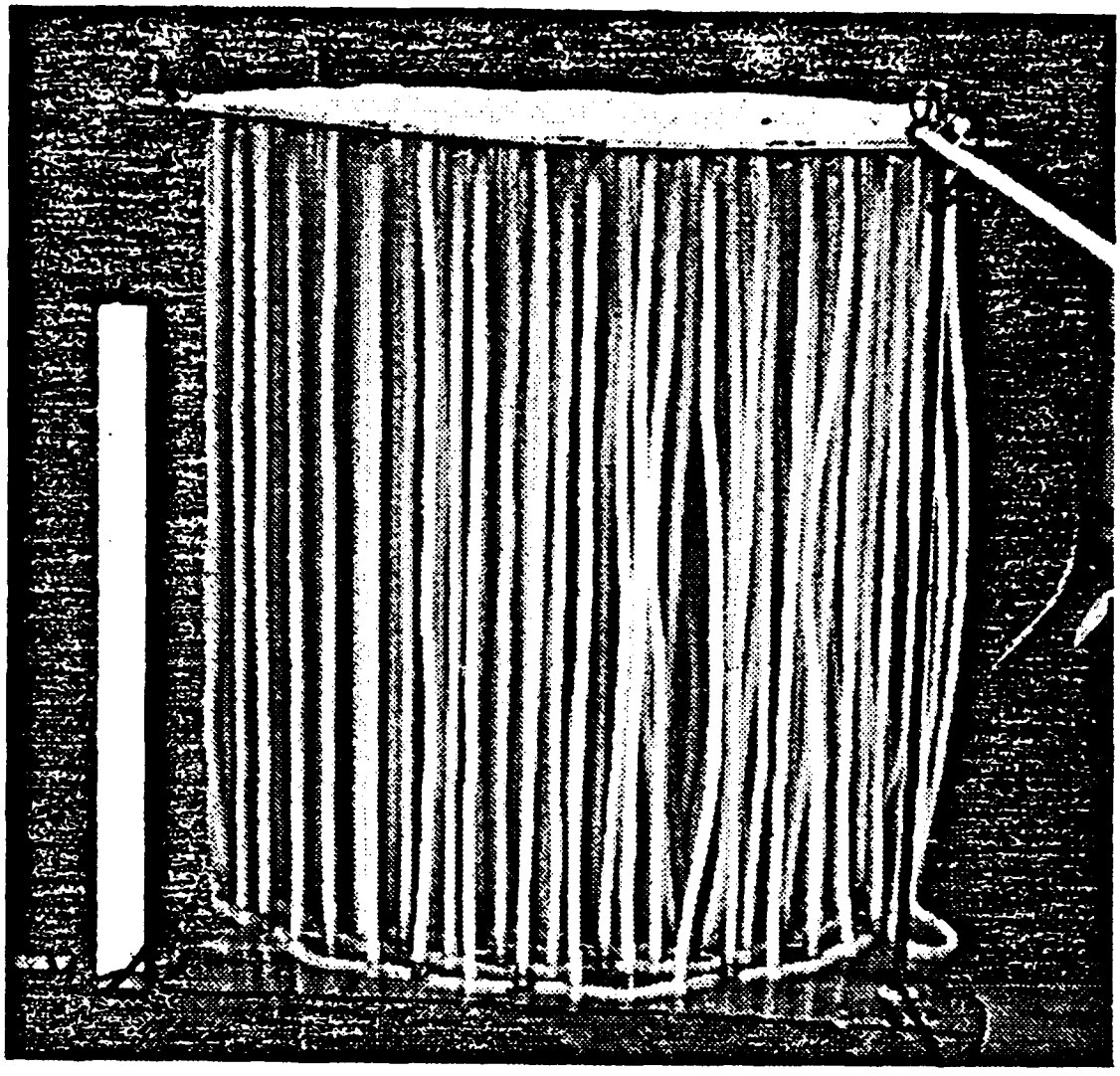

Figure 8. Photo of compliant tube reflector assembly. a=0.19 m, L=0.4 m.

Several reflector models with different numbers of tubes and varied spacing arrangements were built and tested. For this discussion, two representative examples will be described in detail. Both examples had a diameter and length of about 0.4 m (16 in.). Plan views of the tube arrangements are shown in Figs. 9A and 9B.

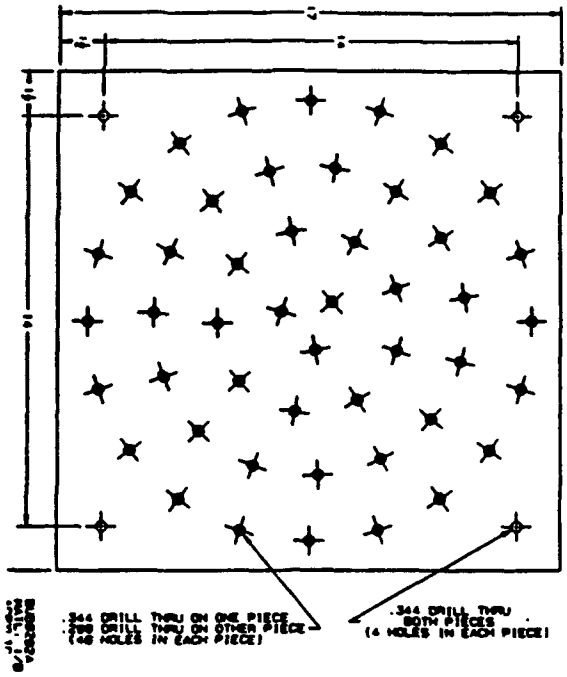

A. 47 tube reflector.

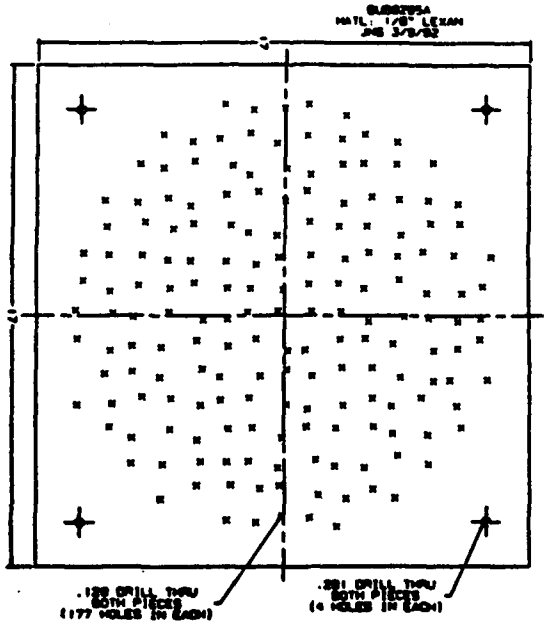

B. 177 tube reflector.

Figure 9. Example tube geometries for multitube reflectors.

The "Mod 2" reflector consisted of 47 tubes, each with a 7.9 mm (5/16 in.) outside diameter (OD), and a 1.6 mm (1/16 in.) wall thickness. The mean tube spacing was 5.6 cm (2.2 in.). The "Mod 3" reflector consisted of 177 tubes, each with a 3.2 mm (1/8 in.) OD, and an 0.8 mm (1/32 in.) wall thickness. The mean tube spacing was 2.5 cm (1 in.). The experimentally-determined resonance frequencies of the 7.9 mm (5/16 in.) OD and the 3.2 mm (1/8 in.) OD tubing were 1300 Hz and 4500 Hz, respectively.

These reflectors were expected to approximate bubble distributions that would give sound speed ratios near 0.2. The fluid sphere theory developed by Anderson (1950) predicted that reflectivity factors of 4 to 5 should be obtained, i.e., the target strength of the test reflector should be 12 to 15 dB higher than that of a rigid sphere (or cylinder) of the same dimensions as the test reflectors. Considering the dimensions of the test reflectors, estimated target strength values ranged from -8 to -6 dB at 2 kHz. The reflector with the 3.2 mm (1/8 in.) diameter tubing was expected to perform better than the reflector with the 7.9 mm (5/16 in.) diameter tubing since it simulated a volume with a more uniform distribution of small bubbles. It also was operating below the resonant frequency of the individual tubes, as required by Anderson's theory.

Measurements of the target strength of these two reflectors in the test tank gave a TS value of -14 dB for the Mod 2 reflector and -24 dB for the Mod 3 reflector at 2 kHz. Since the expected TS values were not obtained, several diagnostic tests were performed. Target strength values predicted by liquid sphere scattering theory depend on reflector penetration by the incident acoustic energy and subsequent multiple scattering from the interior volume. If this did not occur, the test reflectors could act as gas-filled cylinders and scatter most of the incident acoustic energy from the outside surface or they could absorb a significant amount of the incident energy in the interior volume.

A diagnostic experiment was performed in which the interior tubes were removed from the Mod 2 reflector, leaving 20 tubes in the outside cylindrical row. Tests of this configuration gave TS values similar to those obtained for the original full design with 47 tubes. Thus, for this reflector, most of the acoustic energy was evidently being reflected from the outside ring of tubes leaving little energy available for multiple reflections in the interior.

While the Mod 2 reflector had been tested above the resonant frequency of its tube components, the Mod 3 reflector had been tested well below the tube resonant frequency. The low target strength (-24 dB) measured for this reflector assembly showed that sound was probably being absorbed rather than reflected from the interior volume as predicted. By using the relationship ka=.00484 for the fundamental resonance of a gas cylinder in fresh water, the effective radius of the gas inside

the 3.2 mm (1/8 in.) OD tube was only 0.25 mm (1/100 in.) instead of the actual 0.8 mm (1/32 in.). Thus, for the 3.2 mm (1/8 in.) OD tubing, the rubber wall stiffness was apparently dominating the general response and the effective bubble volume was too small to provide enhanced reflectivity. This finding helped to explain the differences observed in the measured target strengths.

3.1.3 Gas-Filled Spherical and Cylindrical Reflectors

The diagnostic test results from the multitube reflectors showed that, at least in scale model tests, it was impractical to produce low sound speed reflectors using small diameter thin wall tubing operating below resonance. The properties of the wall material greatly influenced the general properties of the composite volume. However, if the tubing was operated at and above the resonance frequency the scattering strength was greatly enhanced. Since the test results for the Mod. 2 Reflector showed that the assembly was evidently acting as a gas-filled cylinder rather than a low sound speed fluid volume, the relevant theory for spherical and cylindrical reflectors was reviewed. An analysis published by Stanton (1989) was very helpful in comparing the reflectivity characteristics of gas-filled spheres and cylinders.

Figure 10 shows a comparison of the target strengths of rigid and gas-filled spheres and cylinders. Of particular interest is the comparison of responses below the range where the normalized circumference ka = 1. For rigid reflectors, the target strength decreases at a rate of 12 dB/octave with decreasing ka when the circumference becomes significantly less than a wavelength (ka<1). However for gas-filled spheres and cylinders, The target strength does not fall off appreciably until the value of ka is below the lowest resonant mode of the reflector. At atmospheric pressure in sea water this occurs at ka=.0136 for spheres and at ka=.00478 for cylinders (Weston 1965). As shown in Fig. 10, the resonance of a sphere has a much sharper peak than that of a cylinder. For an undamped gas bubble at atmospheric pressure, the target strength at resonance is 37 dB higher than that for frequencies well above resonance. However, for the gas-filled cylinder it is 17 dB above the target strength at higher frequencies (Weston 1965). The target strength for gas-filled spheres and cylinders remains relatively high for the range of ka values between the lowest resonant mode and the region where ka≥1 because of the excitation of resonant modes in the gas volume (Clay 1991). Because of these modes, gas-filled reflectors produce significantly higher acoustic scattering strength than rigid reflectors below the ka=1 region.

From Eqn.(1) the fundamental resonance of a 1-m radius sphere is 3.2 Hz at atmospheric pressure in sea water. An undamped spherical bubble resonant at 250 Hz under the same conditions would have a radius of 1.3 cm and a target strength of 0 dB. If coherent scattering could be obtained

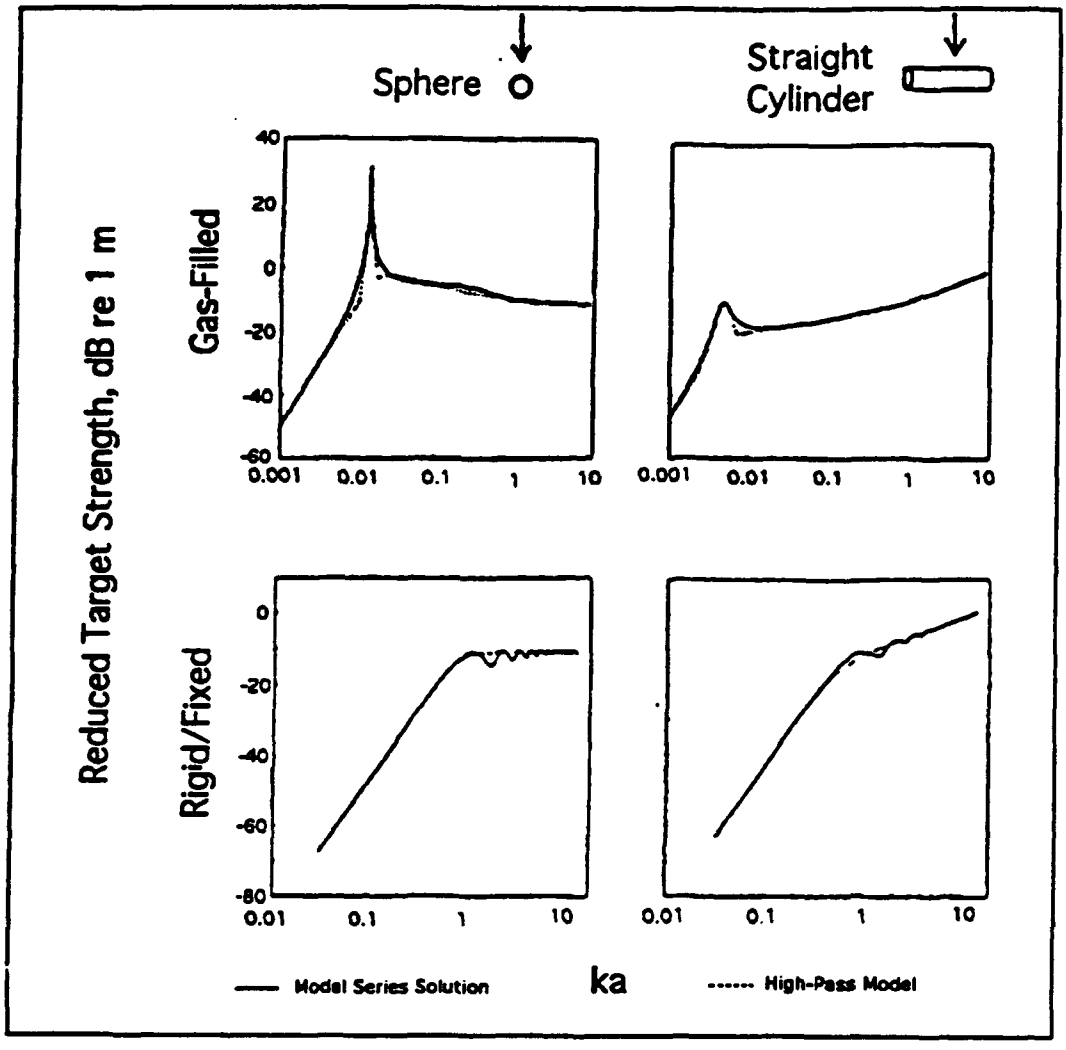

Figure 10. Target strength vs ka for gas-filled spherical and cylindrical reflectors (From Stanton 1988). (Radii and lengths are normalized to 1 m).

from several similarly-sized bubbles, only six bubbles would be needed to produce a target strength of 15 dB. However, if the scattering is incoherent, about 32 bubbles would be needed. The bubbles would need to be constrained to remain in a useful shape, likely requiring a rubber balloon or similar covering material for each bubble. This covering material would introduce damping that would significantly lower the target strength at resonance. The added damping could easily produce a 10-dB loss in target strength, which would require that the number of bubbles be increased to about 320 (assuming incoherent scattering).

A distribution of bubbles with a varied size range would be needed to broaden the effective bandwidth of the resulting reflector. An overriding consideration for a target design involving a

distribution of bubbles is the problem of bubble interaction. This would add significantly to the complexity of the resulting reflector design. After reviewing these design issues for gas-filled spheres, it was decided that the broader resonance and smaller required radius of gas-filled cylinders offered a more attractive alternative for a prototype reflector design.

Directional characteristics were also another important consideration in the reflector design. In most anticipated applications, the reflector will have sound arrival angles near horizontal incidence and will need to provide either backscattered returns or bistatic returns in the horizontal plane. In this application a vertically oriented cylinder reflector would be beneficial because of its innate vertical directional properties. Moreover, as shown by Stanton's analysis, a cylinder with ka<<1 provides an omnidirectional horizontal bistatic scattering pattern that would be useful for calibrated target strength applications.

3.2 Sound Scattering from Finite Cylinders

The suitability of gas-filled cylinders for the reflector design was investigated by using Stanton's analysis to develop a computer-based model for predicting target strength values for selected ranges of relevant parameters. Calculated target strength curves were generated for the experimental reflectors using this model. The computer model was also used to produce generic target strength curves for gas-filled cylinders at depths of 10, 30, and 100 m. These curves are presented in Appendix A.

Stanton (1988)[4] gives the scattering amplitude function for a finite cylinder as

$$f(\Omega) = \left(-\frac{iL}{\pi}\right)\frac{\sin(kL\cos\theta)}{kL\cos\theta}\sum_{m=0}^{\infty} B_m(-i)^m\cos(m\phi) \qquad (2)$$

where Ω = spherical angles

L = cylinder length (m)

θ = incidence angle in the plane of the cylinder axis ($\theta = \pi/2$ for broadside incidence)

B_m = a coefficient involving Bessel Function computations

ϕ = scattering angle in the plane normal to the cylinder axis ($\phi = \pi$ for backscatter)

m = Bessel Function order number

[4] The reader is referred to Stanton (1988) for a complete derivation of the scattering function given in this analysis. Stanton also developed "simplified" target strength calculation procedures, adapted from high-pass filter theory, which do not require Bessel Function computation. The dotted curves in Fig. 10 were produced by this approximate method.

The target strength as defined by Urick (1983) can be determined as

$$TS = 10\text{Log}_{10}\left|f(\theta, \phi = \pi)\right|^2 \text{dB} \tag{3}$$

For normal-incidence backscattered sound at the fundamental resonance of the cylinder (m=0), Eqn. (2) evaluates as

$$f\left(\theta = \frac{\pi}{2}, \phi = \pi, m = 0\right) = -\frac{iL}{\pi} \tag{4}$$

As a result, the target strength for a long, gas-filled cylinder at resonance becomes simply

$$TS = 20\text{Log}_{10}\left(\frac{L}{\pi}\right)\text{dB} \tag{5}$$

This equation does not consider bubble wall damping effects and depth pressure effects that will act to reduce the achievable target strength.

3.3 Test Results Compared with Theory

The computer model based on Stanton's analysis was used to obtain predicted target strength curves for scale model and full scale reflectors. Calculated curves were obtained showing frequency dependence for backscatter (monostatic) geometry as well as horizontal and vertical bistatic directivity patterns.

3.3.1 Backscatter (Monostatic) Geometry

The data obtained for tests of the multitube reflectors and for tests of a single tube are compared with a calculated target strength curve in Fig. 11. General agreement between the data and theoretical predictions encouraged development of the cylindrical reflector design in an attempt to reach the design goal of 15 dB at 250 Hz. Of particular significance, as noted above, was that the target strength values of a cylinder at or near resonance at ka=0.005 equal those obtained for a cylinder with a diameter 200 times larger, operating near ka=1. As shown in Fig. 11, the target strength values are not reduced significantly at frequencies well above resonance, supporting the design goal of broad band operation. Moreover, for ka<1 the normal incidence target strength of a long cylinder does not increase with frequency at 6 dB per octave as does the output of a linear transducer array.

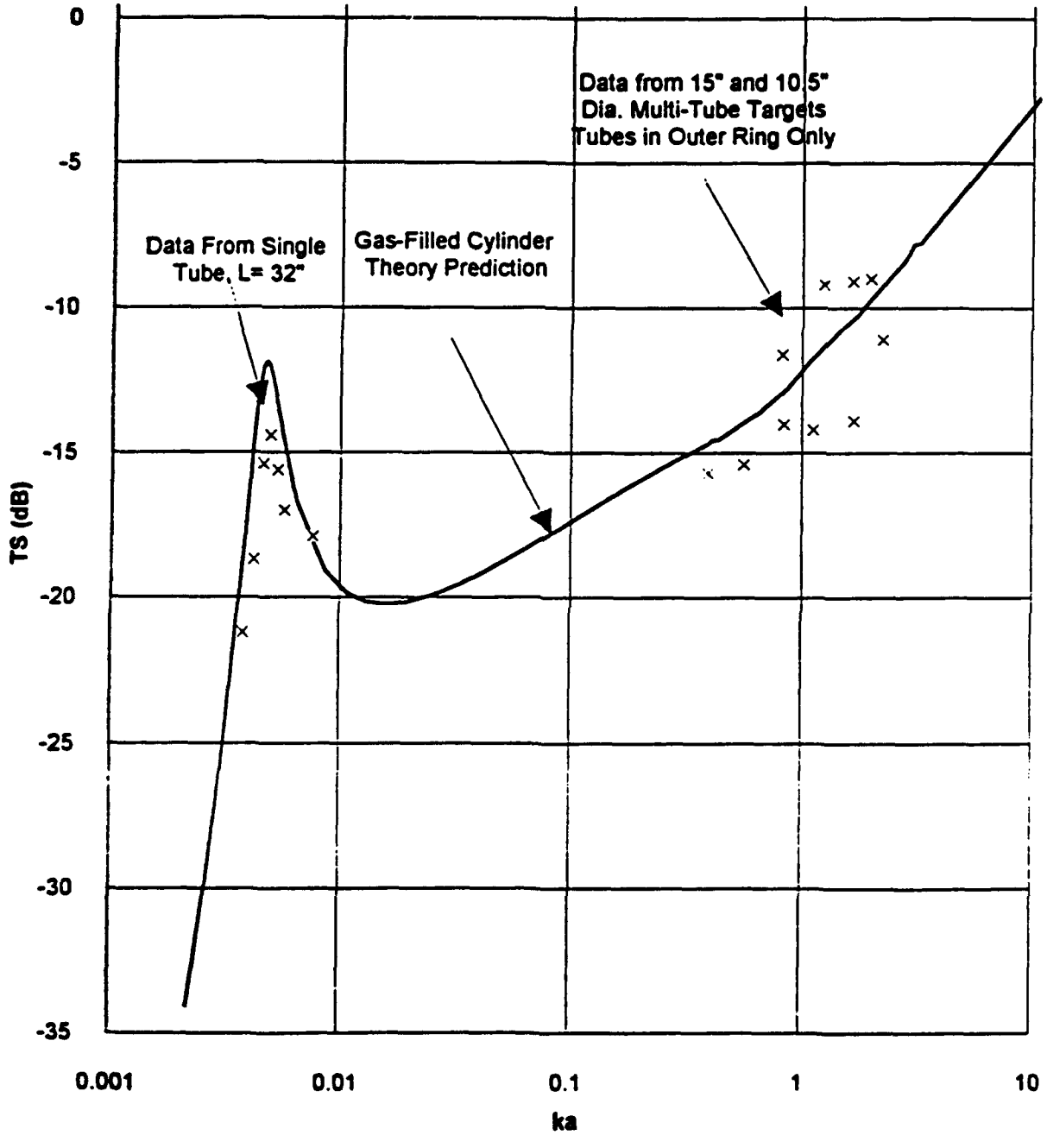

Figure 11. Target strength vs ka, single and multi-tube model reflectors, gum rubber tubing dim. OD 7.9 mm (5/16 in.), wall 1.6 mm (1/16 in.), length 0.81 m (32 in.).

An explanation for this apparently anomalous behavior can be found in an analysis by Weston (1965). His analysis of the scattering strength of linear arrays of spherical bubbles showed the effective scattering strength of an infinite linear array of spherical bubbles to be identical with that of a cylindrical bubble of the same radius when the individual bubble spacing was less than $\pi/2$. The resonance frequency of the individual bubbles was lowered to that of a cylindrical bubble because of the interaction of the pressure fields between the bubbles that become stronger with increasing proximity. Near resonance, the effective scattering cross section/unit length of the cylindrical array was much larger than the actual width of the bubbles. Weston stated it was equivalent to a strip area of width,

$$a=\lambda/\pi \quad (m) \tag{6}$$

extending on either side of the cylinder axis. This is the result of the extended influence of the pressure release effect of the flow field around the bubble. As a result, the width of the effective cylinder is proportional to the wavelength. Thus, as the effective acoustic length (L) of the cylinder increases with frequency , the effective acoustic width ($2\lambda/\pi$) decreases, keeping the scattering cross section relatively constant until the $ka \geq 1$ region is reached. In this region the effective modal response width becomes insignificant compared to the actual cylinder width and the target strength begins to increase at 3 dB/octave as shown previously in Figs. 10 and 11. This characteristic is observed for both gas-filled and rigid cylinders and is given by the relationship (Urick 1983)

$$TS = 10\ Log_{10}(aL^2/2\lambda)\ (dB) \tag{7}$$

Weston's results shown in Eqn. (6) suggest that the effective ka of the gas-filled cylinder at resonance is 2. Since Eqn. (7) is valid for $ka > 1$, we can combine this equation with Eqn. (5) from Stanton's analysis to obtain a second estimate of the effective cylinder radius at resonance. This becomes

$$a = 2\lambda/\pi^2 \quad (m) \tag{8}$$

which is smaller than Weston's result[5]. Using Eqn. (8), the value of ka at resonance becomes $4/\pi$ or 1.27. This analysis result is supported by the calculated curve shown in Fig. 11 where the target strength at resonance is equal to the value at $ka \approx 1.3$.

[5] If the scattering cross section/unit length of the gas-filled cylinder is considered to be equal to 1/2 of the circumference (πa), rather than the cylinder width ($2a$), then this result is equivalent to Weston's.

The calculated curve in Fig. 11 shows that the target strength of a cylindrical bubble at shallow depths remains within an envelope ±4 dB wide from $.004 \leq ka \leq 1$; suggesting that the relationship developed in Eqn.(5) for a cylindrical bubble near the fundamental resonance can also be applied approximately at higher frequencies.

Stanton (1989) developed empirical relationships for predicting the target strength for several classes of finite cylinders. These "simplified" relationships do not require Bessel Function computations as in the exact analysis. Stanton's equations were combined with data reported by Clay (1991) for the depth dependence of gas-filled cylinder scattering to obtain an empirical procedure for calculating the target strength of a gas-filled cylinder as a function of depth. This procedure and some sample results are included in Appendix A.

3.3.2 Bistatic Geometry

Bistatic scattering strength data were obtained using the 20-tube version of the reflector shown in Fig. 9A (only outer ring filled). Tests were made using two configurations, each with a radius of 0.19 m, but varied lengths of 0.4 m and 0.8 m. A photo of the 0.8 m length configuration is shown in Fig. 12. The data obtained are compared with the model predictions for the 0.8 m length in Fig 13A. The agreement can be seen to be good with the data showing slightly higher values than the predicted results. The forward scattering strength is about 7 dB higher than the backscattering strength for this diameter reflector (ka=1.6). Equation (7) predicts that the target strength for the 0.4 m long reflector should be 6 dB less than that of the longer configuration. The data shown in Fig. 9A support this prediction with some experimental scatter.

Bistatic scattering strength data were also obtained using one of the individual tubes from the 20 tube reflector. The frequency dependence of the backscattering strength of this tube was shown previously as the single tube data in Fig. 11. The bistatic data shown in Fig. 13B agree well with the predicted curve from the computer model. Theory predicts an omnidirectional bistatic scattering pattern for cylindrical reflectors when $ka<1$, as confirmed by the results shown in Fig. 13B (at 2 kHz $ka \approx 0.0074$ for this tube). At 2 kHz the target strength of the single tube is 8 dB lower than that of the 20-tube reflector for backscatter incidence.

Equation (5) shows that if the length of the single tube reflector was increased to 2m, it would have the same target strength as the 20-tube reflector at normal incidence. The computer model was used to calculate the target strength characteristics of the longer single tube since the dimensions of the BBN test tank did not permit an experimental test of a target 2 m long. The vertical bistatic scattering pattern was of particular interest since increasing the length of the tube produces a narrower scattering pattern in the plane of the cylinder axis. A long single tube thus can provide a

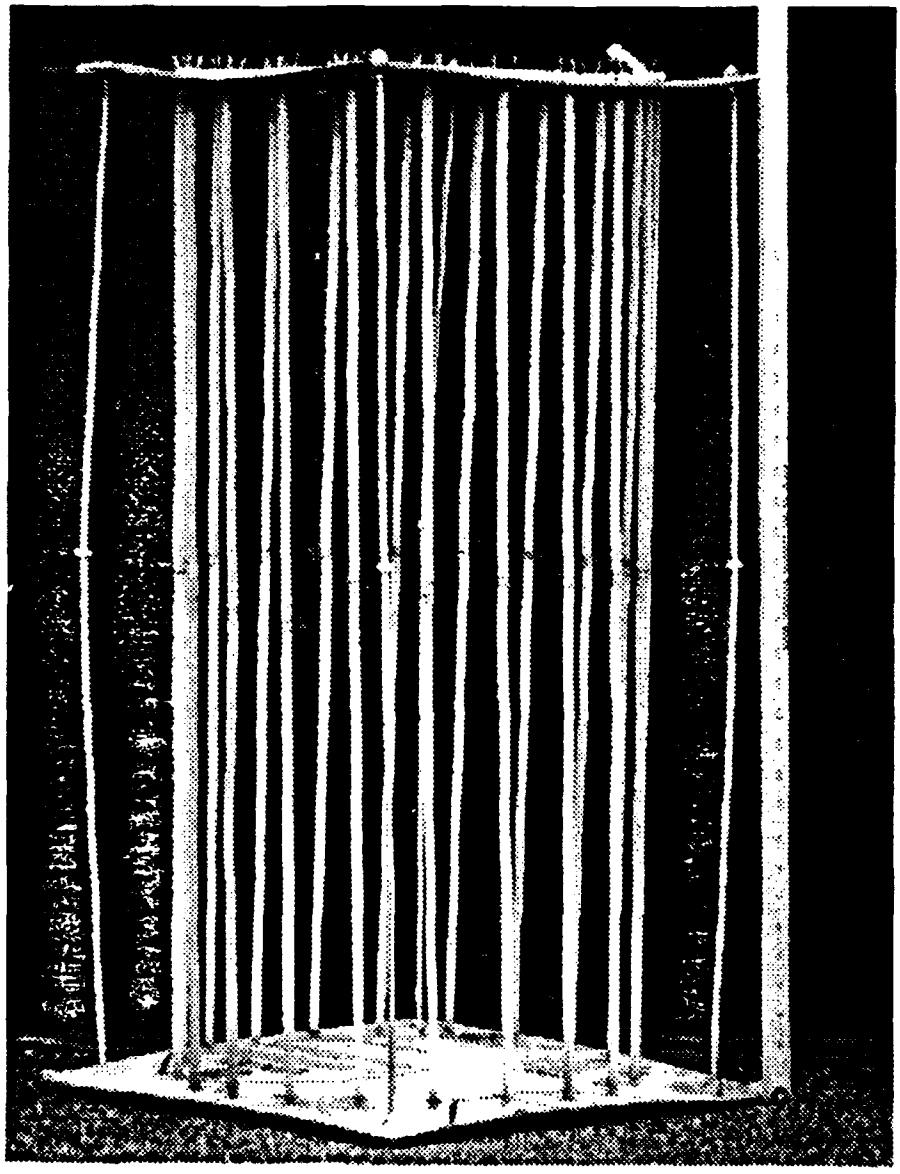

Figure 12. Photo of 20 tube reflector, a=0.19 m, L=0.8 m.

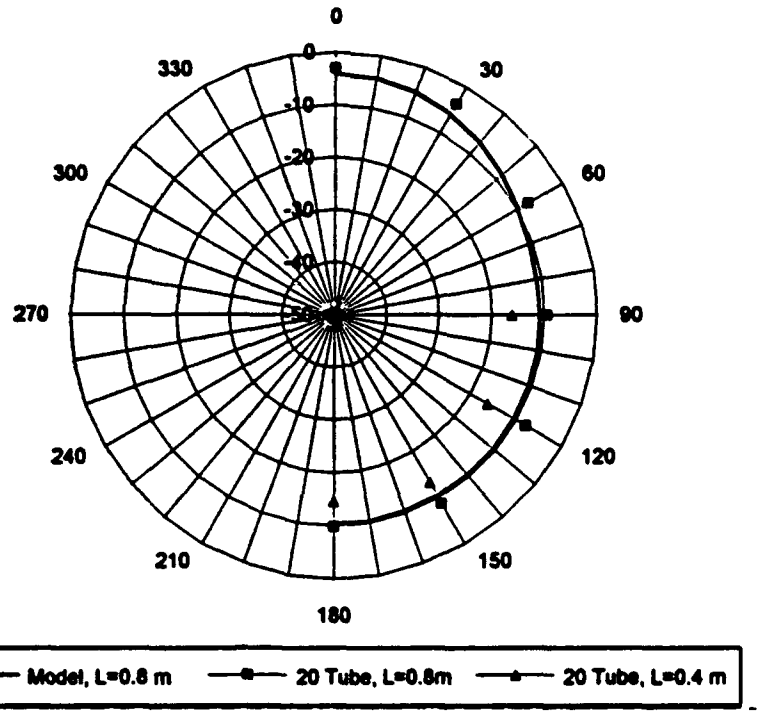

A. Data compared with model prediction for gas-filled cylinder, a=0.19 m, 2 kHz.

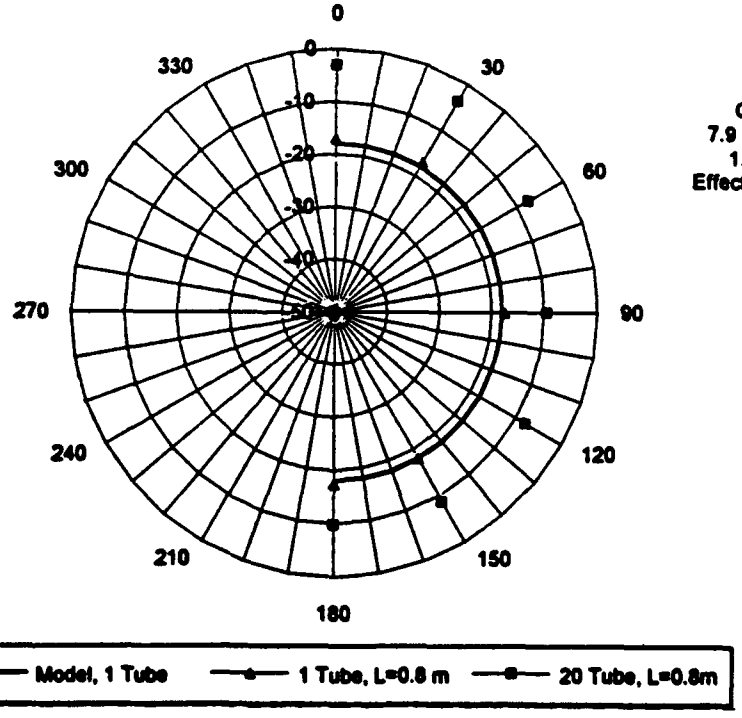

Gum Rubber Tubing
7.9 mm (5/16 in) Diameter
1.6 mm (1/16 in) Wall
Effective radius, a = 0.85 mm

B. Data for 20 tube, a=0.19 m, compared with 1 tube, a=0.85 mm, 2 kHz.

Figure 13. Bistatic target strength for tube reflector.

more efficient reflector design than a short group of multiple tubes if the resulting narrower vertical reflectivity pattern is acceptable.

The results of vertical bistatic scattering calculations for the single tube, 2 m reflector and the 20-tube, 0.8 m reflector are shown in Fig. 14. In this figure, 90° represents backscatter aspect, and 0° scattering toward the surface. The backscatter target strength for the two reflectors can be seen to be equal as expected. The scattering pattern for the 20-tube reflector is broader than that of the single tube, having an effective beamwidth (6 dB down) of 135°, vs 26° for the single tube. However, in the ocean environment the expected sound incidence angles for the full-scale reflector are expected to be nearly horizontal. A 26° scattering beamwidth was considered acceptable and was used to define the length scaling limit for the full scale design.

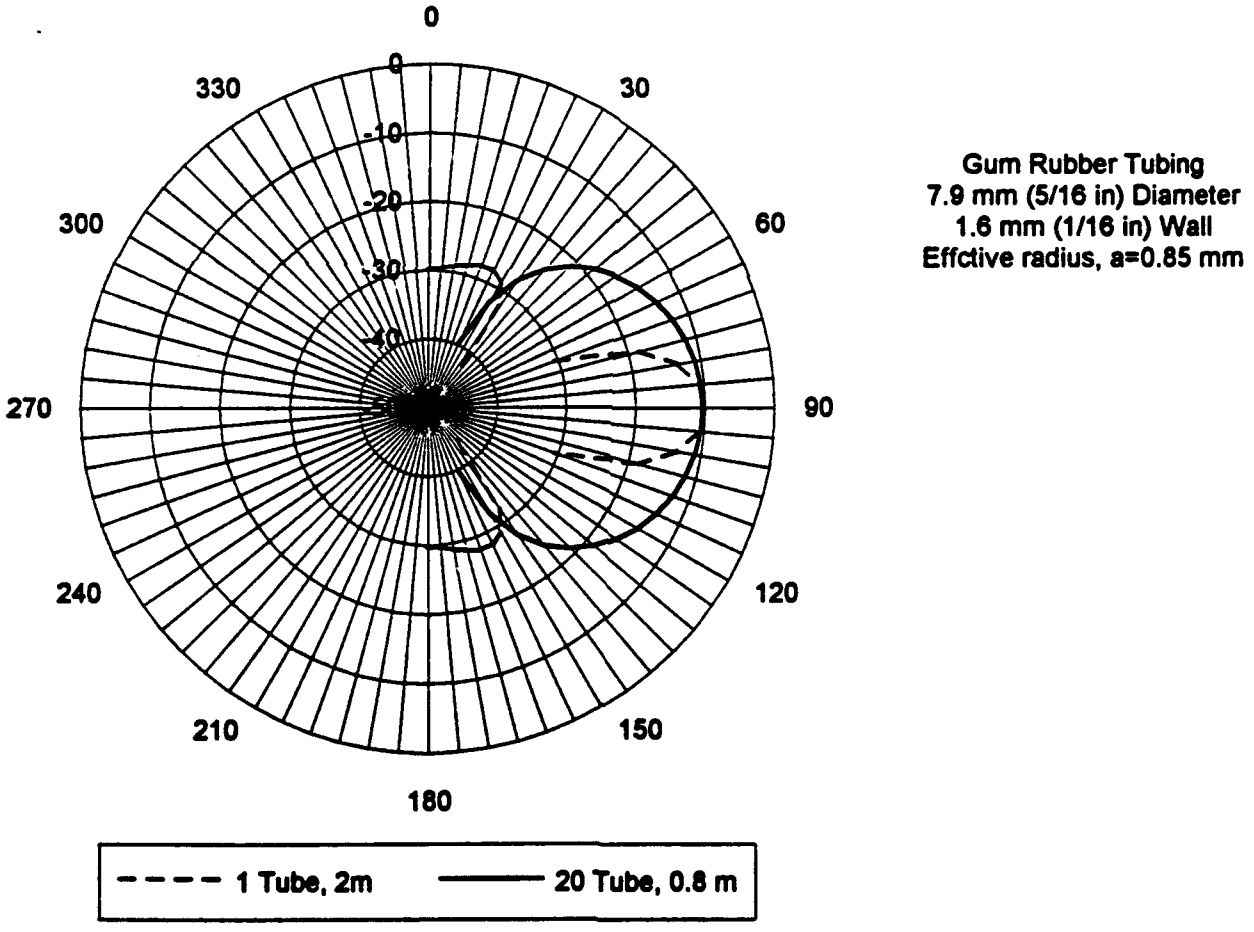

Figure 14. Bistatic target strength for tube reflector. Vertical scattering pattern for normal incidence, 20 tube, a=0.19 m, compared with 1 tube, a=0.85 m.ก, 2 kHz.

3.3.3 Multiple Cylinder Scattering

The multiple tube reflector tests described previously in Section 3.1.2 involved designs wherein the tube spacing was a small fraction of a wavelength to minimize irregularities in the reflector scattering pattern caused by interference between the scattering patterns of individual tubes. The analysis presented in Section 3.2 showed that near the resonant frequency of n gas-filled cylinder the effective scattering diameter is about 0.4λ. A row of tubes spaced up to 0.4λ apart should thus act as a continuous gas-filled layer for frequencies near and above the tube resonance. This was confirmed by Toulis (1957) who reported test results for compliant metal tube arrays showing that linear tube spacings <λ/2 provided acoustic properties similar to those of a continuous air layer. Tests were performed to check this prediction using air-filled rubber tubing and investigate the effects of variations in spacing and geometry for two and three tube multiple reflector combinations. In all tests the orientation of the tubes was vertical and only the horizontal bistatic incidence angle was varied.

Two Tube Results. The target strength for two tubes at broadside incidence was measured for varied tube spacing using pulse frequencies above and below the individual tube resonance. For spacing > λ/2, where the hydrodynamic fields do not interact, coherent reflections from two equidistant tubes would be expected to produce a 6 dB increase in target strength. The results (Fig. 15) show that, as expected, the target strength increased with increasing tube spacing with an increase of 4 to 5 dB in target strength occurring for spacings of λ/4. The test results at 1.5 kHz show higher target strengths at even shorter spacing probably because of the proximity of the test frequency to the individual tube resonance near 1.3 kHz (see Fig. 11).

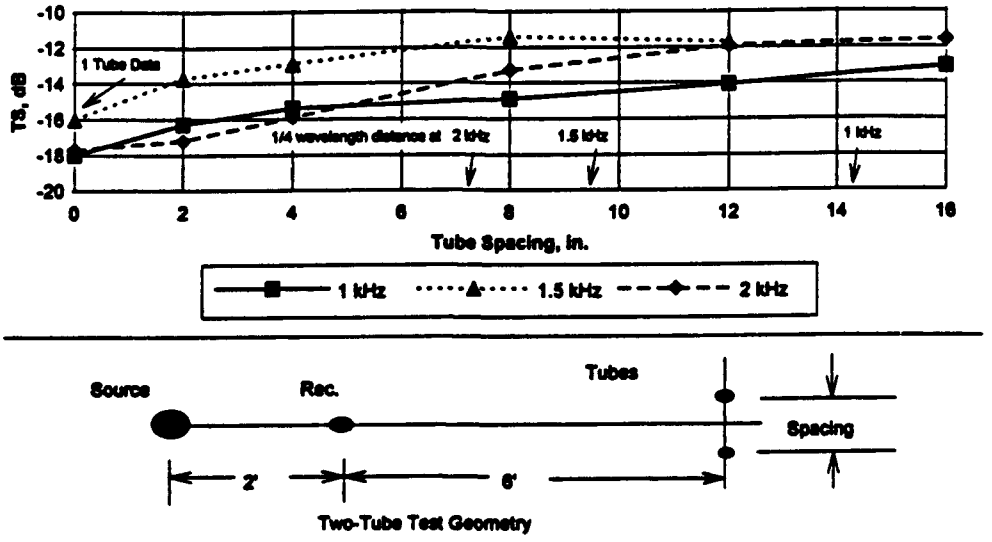

Figure 15. Target strength for two tubes vs separation distance, tubing OD=7.9 mm (5/16 in), L=0.8 m (32 in) (see sketch).

A comparison of two tube target strengths as a function of spacing was made at 2kHz for both broadside and axial incidence as shown in Fig. 16. The results show that for axial incidence a significant reduction in target strength occurs at a spacing of 8 in (0.2 m). This corresponds to a spacing of about $\lambda/4$ (see Fig. 15) which would be expected to produce destructive interference between the reflected signals at the test frequency. Comparison of the target strengths for broadside and axial incidence at this spacing shows that the horizontal bistatic target strength pattern would have about a 7 dB variation.

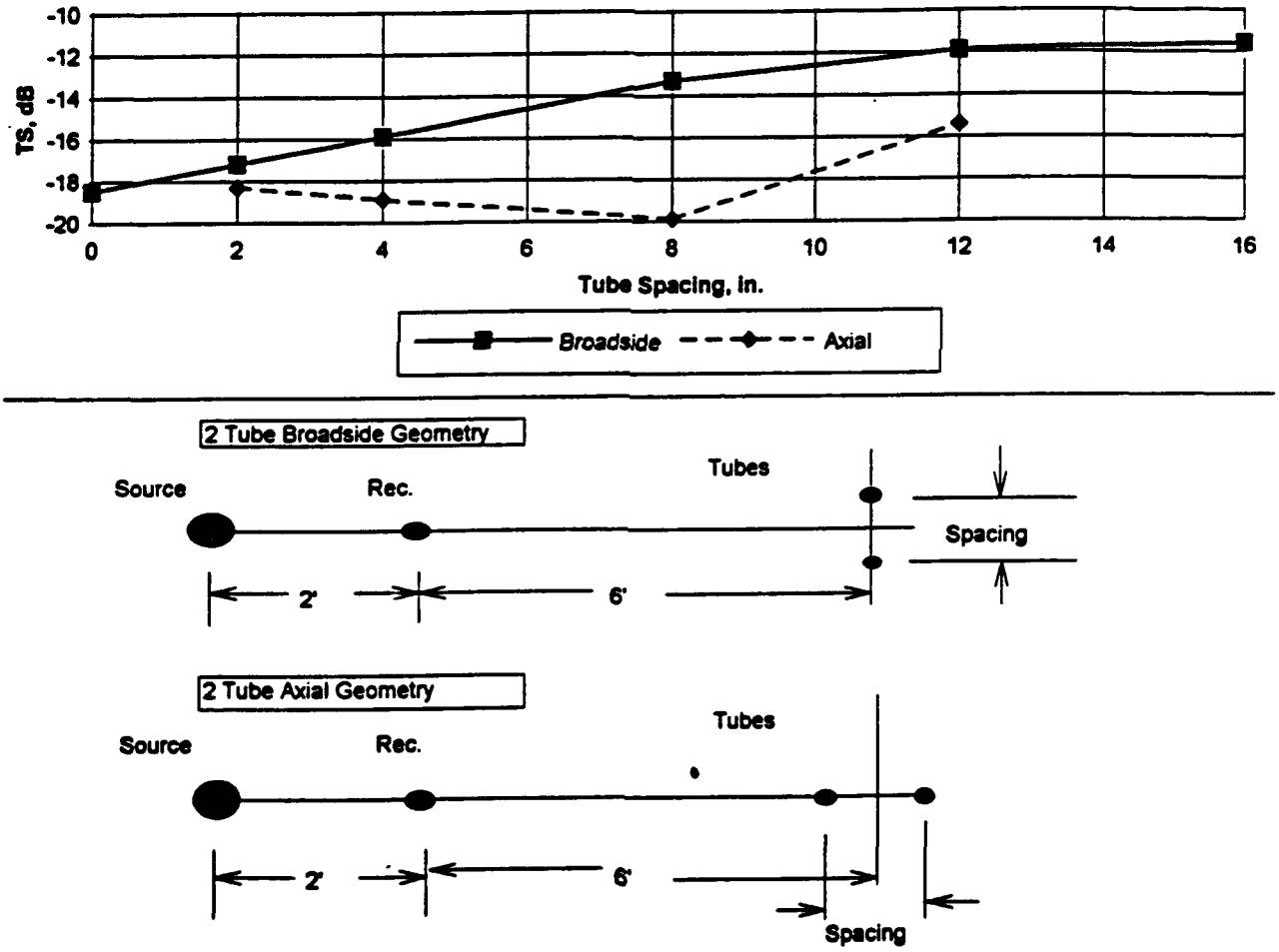

Figure 16. Target strength for two tubes vs separation distance, broadside and axial geometries, f=2 kHz (see sketches).

Three Tubes. A test of a three-tube reflector was made at 2 kHz using the geometry shown in Fig. 17. Two tubes spaced at about $\lambda/2$ were placed in a fixed orientation at broadside incidence with a third tube at varied positions along the sound path. The target strength expected for this combination of equidistant coherent reflectors would be 9.5 dB higher than that of single reflector or about -8.5 dB in this case. Figure 17 shows that a value of -9.5 dB is obtained when the three tubes are in line and drops only slightly when the center tube is moved 4 in. (0.1 m) toward the source. However, when the third tube is moved away from the source the target strength drops more rapidly, approaching the target strength for two tubes alone for an offset of 4 in. When the offset is increased to 8 in. (0.2 m), the target strength drops to less than that of a single tube.

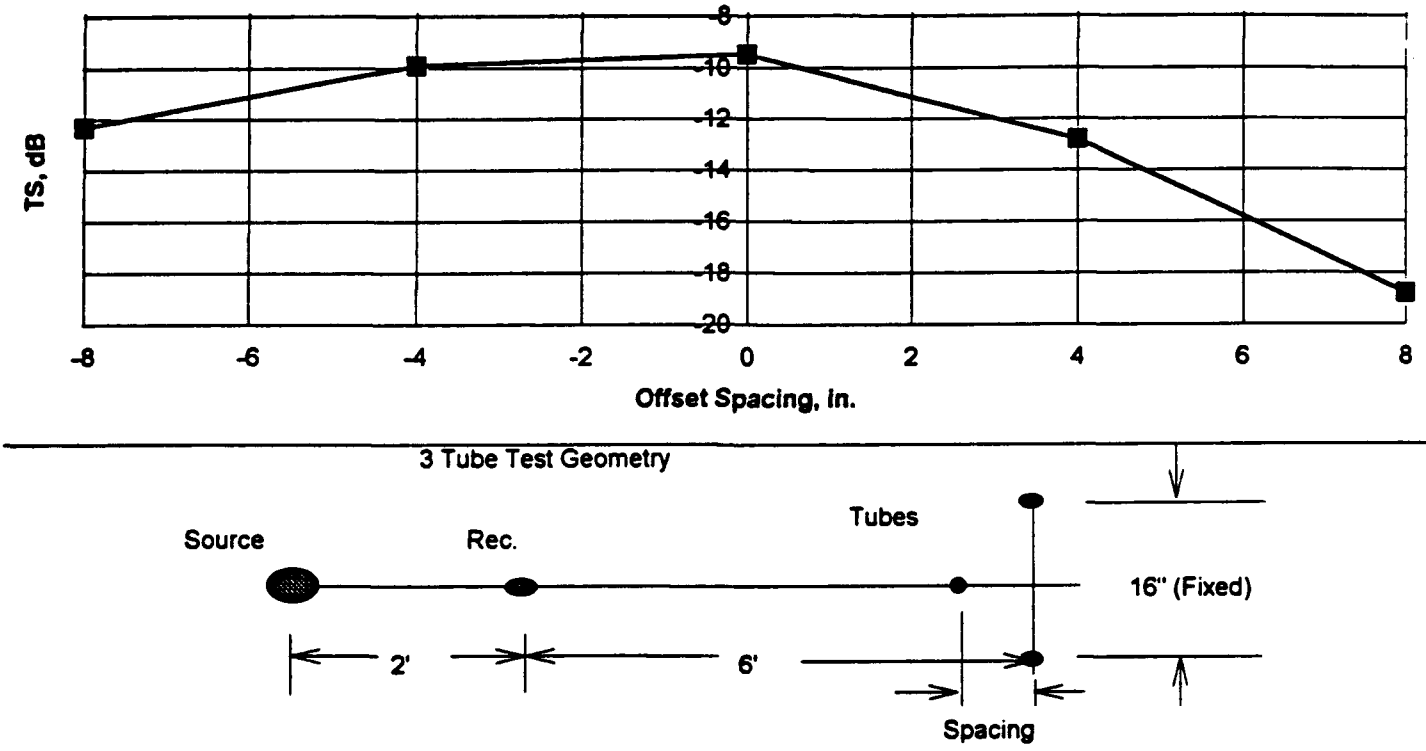

Figure 17. Target strength for three tubes vs center tube offset distance, f=2 kHz (see sketch).

In applying these results to multiple tube reflector design, it is apparent that in the case of the cylindrical design with interior tubes, the inside tubes were generally not inhancing the overall target strength. They may have been actually reducing it because of destructive interference effects.

4. FULL-SCALE REFLECTOR DESIGN

As shown previously in Fig. 11, the test results with the model multitube reflectors provided only a modest increase in target strength over the single tube reflector operated near resonance. Thus the advantage of simplicity weighed heavily in favor of testing the suitability of a single tube for the full-scale design.

4.1 Length Considerations

Theoretically, the target strength goal could be achieved by simply selecting the length of the tube and the desired resonant frequency. Equation (5) gives a required length of 17.7 m to achieve a target strength of 15 dB. However, the effect of the tube length on the vertical scattering pattern must also be considered as discussed previously. If the tube is too long the vertical pattern will be very narrow and sound incident at angles oblique to the cylinder axis will not be backscattered but will be scattered primarily at the specular reflection angle. Also it will be difficult to maintain vertical alignment over the length of the cylinder in the presence of current shear. The design beamwidth goal of 26° (6 dB down) was selected after considering the probable acoustic arrival angles in most deployment areas. This permitted a reflector length of 16 m at 250 Hz, based on predicted beam patterns using the target strength model developed from Stanton's analysis. Shortening the tube reduced the calculated TS value at resonance to 14 dB. This was regarded as an acceptable compromise.

4.2 Tube Radius

The required radius to achieve resonance at 250 Hz is influenced by the planned operating depth and by the properties of the material used to contain the cylindrical bubble. Gum rubber tubing was selected because of its relatively low elastic modulus and because of its commercial availability. A previously developed BBN computer model (ARMAC) capable of calculating the target strength of composite, multilayered cylinders, was used to calculate the target strength of several sizes of gum rubber tubing to determine suitability for use in the full-scale reflector. The tubing dimensions were driven not only by the resonance frequency requirement but also by the need to withstand a depth pressure gradient of around $1.59X10^5$ Pa (23 psi) over the vertical length of the tube. A commercially-available gum rubber tubing with a 5.7 cm (2 1/4 in.) OD and a 1.3 cm (1/2 in.) wall was found to be capable of withstanding an inflation pressure of at least $1.72X10^5$ Pa (25 psi). The predicted target strength of a 16 m length of this tubing (Fig. 18) was 13 dB at a resonance frequency of 320 Hz for an operating depth of 91 m (300 ft). This predicted TS characteristic was considered acceptable for the prototype reflector since the tests planned for the unit would use broad band sound sources.

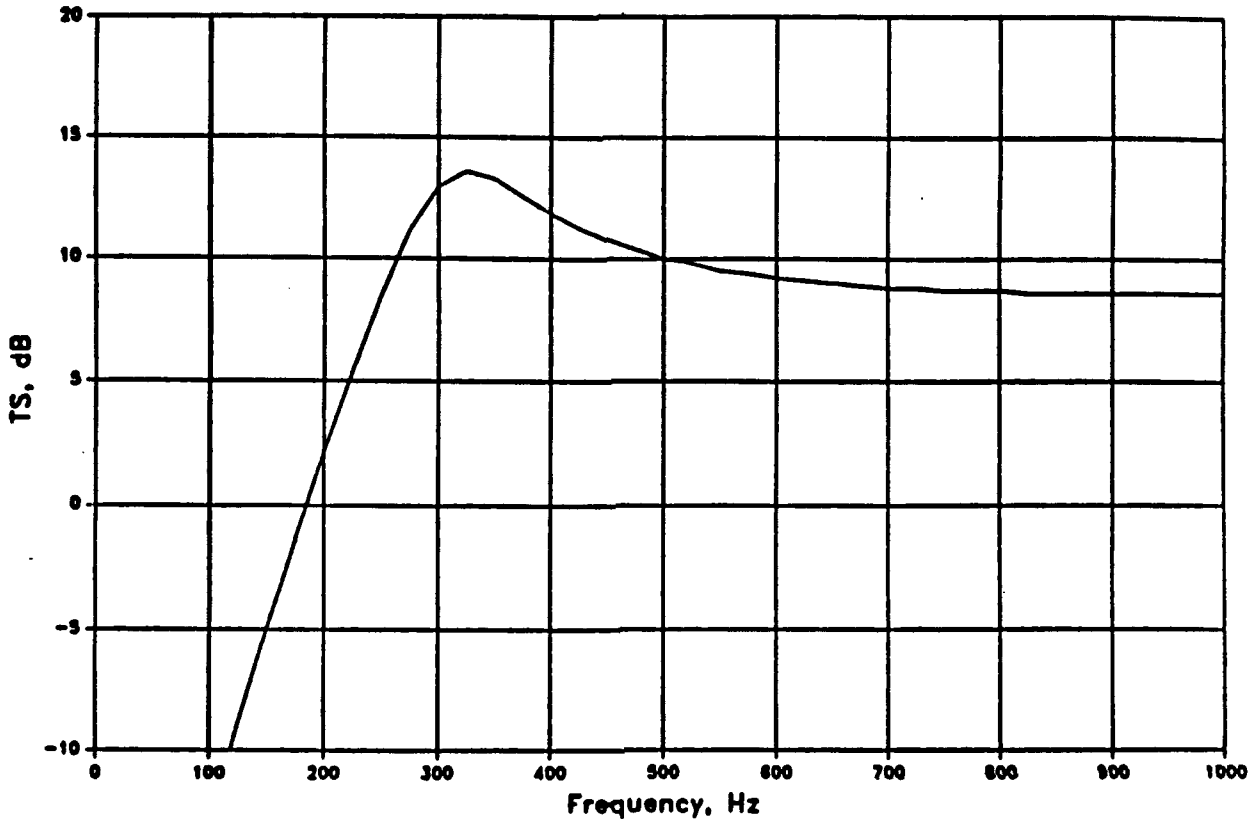

Figure 18. Target strength vs frequency for full scale reflector, gum rubber tubing, OD 5.7 cm (2 1/4 in.), wall 1.3 cm (1/2 in.) length 16 m (52.5 ft).

4.3 Prototype Reflector Description

The high target strength tubular reflector prototype shown in Fig. 19 consists of a length of flexible tubing pressurized by means of an automatic inflation valve from a gas cylinder (A SCUBA regulator and standard dive tank are used in the prototype). A central strength cable is passed through the center of the tube to provide a means of tensioning to a controlled length during deployment (The prototype unit has a deployed length of 17 m, including three nonreflective hose couplings). Tensioning force is provided by a float attached to the top of the tube assembly and a ballast weight or anchor attached to the bottom. (The prototype was deployed using a mid-depth float with 17.3 kg (38 lb.) buoyancy.) The reflector tube has an additional buoyancy of about 16 kg (35 lb.) so that the ballast weight/anchor must be sized to counteract this buoyancy and provide sufficient additional force to maintain position in the presence of current drag forces that may be present in the installation area.

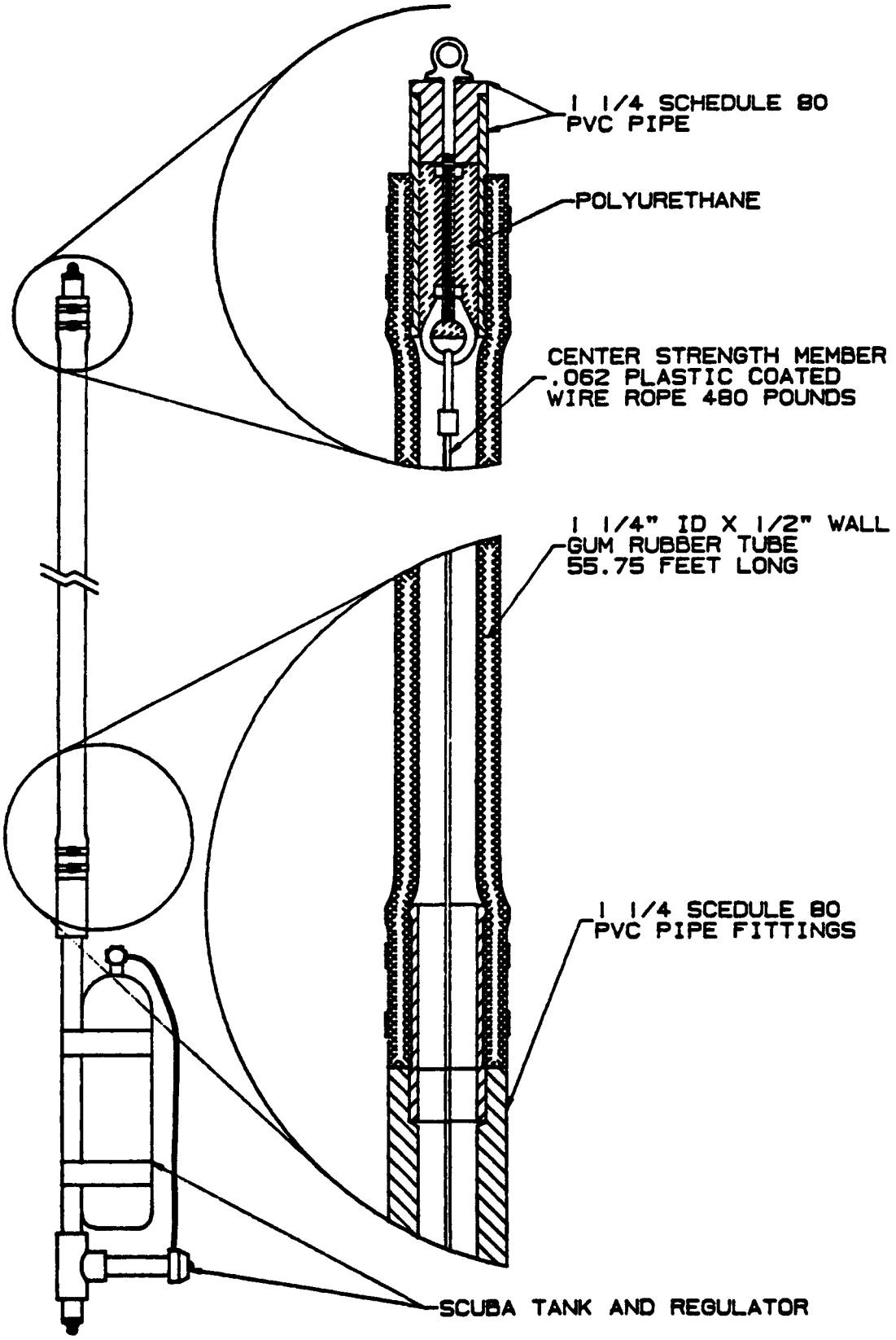

Figure 19. Prototype reflector assembly.

4.4 Test Results

The prototype unit shown in Fig. 19 was field tested during a DARPA-sponsored low frequency active sonar trial in the Gulf of Mexico (ACT-1). The unit was deployed as shown in Fig. 20 and tested using impulsive sound sources. The echo signal from the reflector was received on a beamformed horizontal array deployed near the bottom. A representative echo signal is shown on a beamformed output display in Fig. 21. The results of tests using both monostatic (backscatter) and bistatic geometries are summarized in Table 1.

Table 1. Full-Scale Target, ACT-1 Test Results

	Monostatic Test	Bistatic Test
Range	9.3 km (5 nm)	Source-Target 15.8 km (8.5nm) Target-Receiver, 9.3 km (5 nm)
Target Strength @ freq	260 Hz	260 Hz
Mean	11.1 dB	13.2 dB
S.D.	2.0 dB	2.3 dB
Scatter	9-14 dB	10.5-17.5 dB
N	7 impulses	6 impulses
Echo BW	100-400 Hz	

A second prototype reflector, using the same design as shown in Fig. 19, was assembled and tested at the NUWC Lake Seneca Facility. A shorter, 4-m reflector was also tested because of far-field measurement distance limitations at the facility with the full-scale reflector[6]. Measurements were made of backscatter target strength and vertical directivity patterns. The results of the backscatter tests on the full-scale reflector are compared with the calculated target strength curve in Fig. 22. A peak TS value of 12 dB was obtained at 250 Hz. To extend the frequency range of the data, the shorter 4-m target was used with the results also shown in Fig. 22. The agreement with the calculated curve is good except at higher frequencies. It is believed that the lower values of TS were observed because of target deflection due to current drag. Current-induced tilt would reduce the apparent target strength at high frequencies because the narrower beam pattern would be tilted away from the horizontal.

The vertical directivity of the full-scale reflector was tested at 250 Hz for sound arriving at normal incidence to the target axis (90°) and sound arriving at oblique incidence (70°). The resulting data are compared with calculated patterns in Fig. 23. The TS values on the backscattered beam axis

[6] Where appropriate, the measured data were adjusted to compensate for near field measurement locations. The analysis involved is presented in Appendix B.

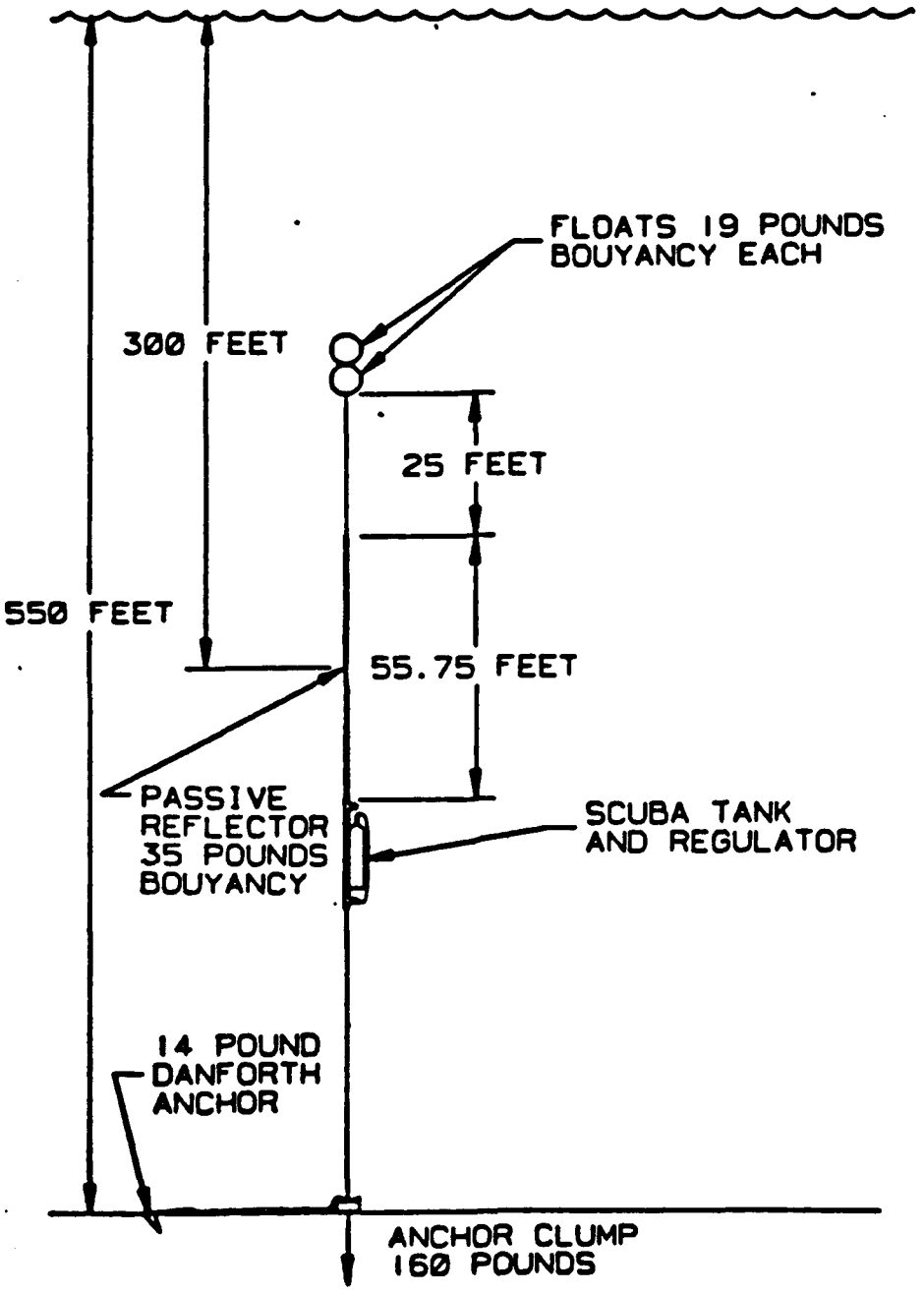

Figure 20. Reflector deployment arrangement for ACT-1 Test.

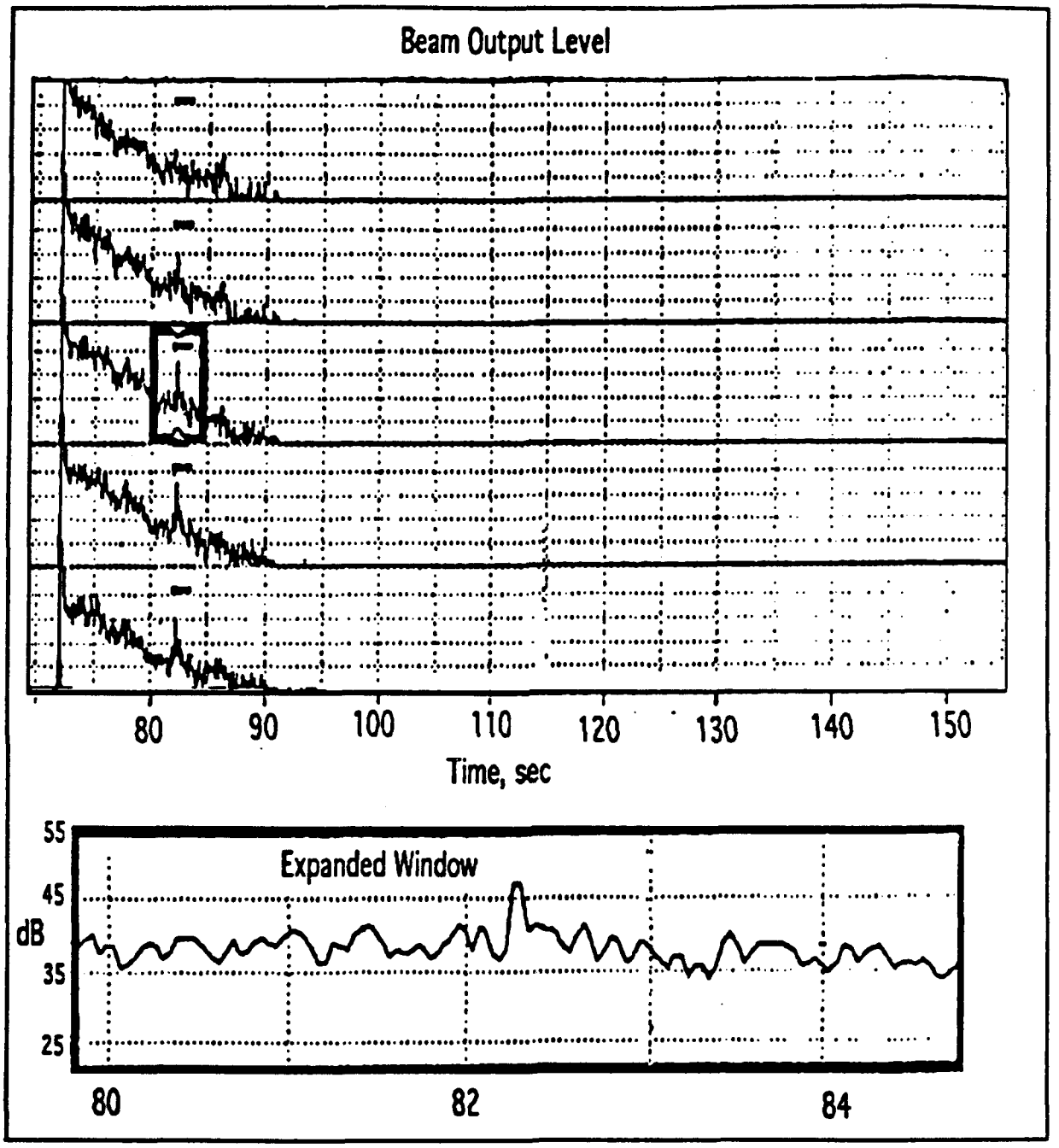

Figure 21. Beamformed array output showing reflector echo detection. Target range - 9.3 km (5 nm), Water depth 180 m (600 ft), Analysis BW 200-350 Hz, Integration Time 20 msec.

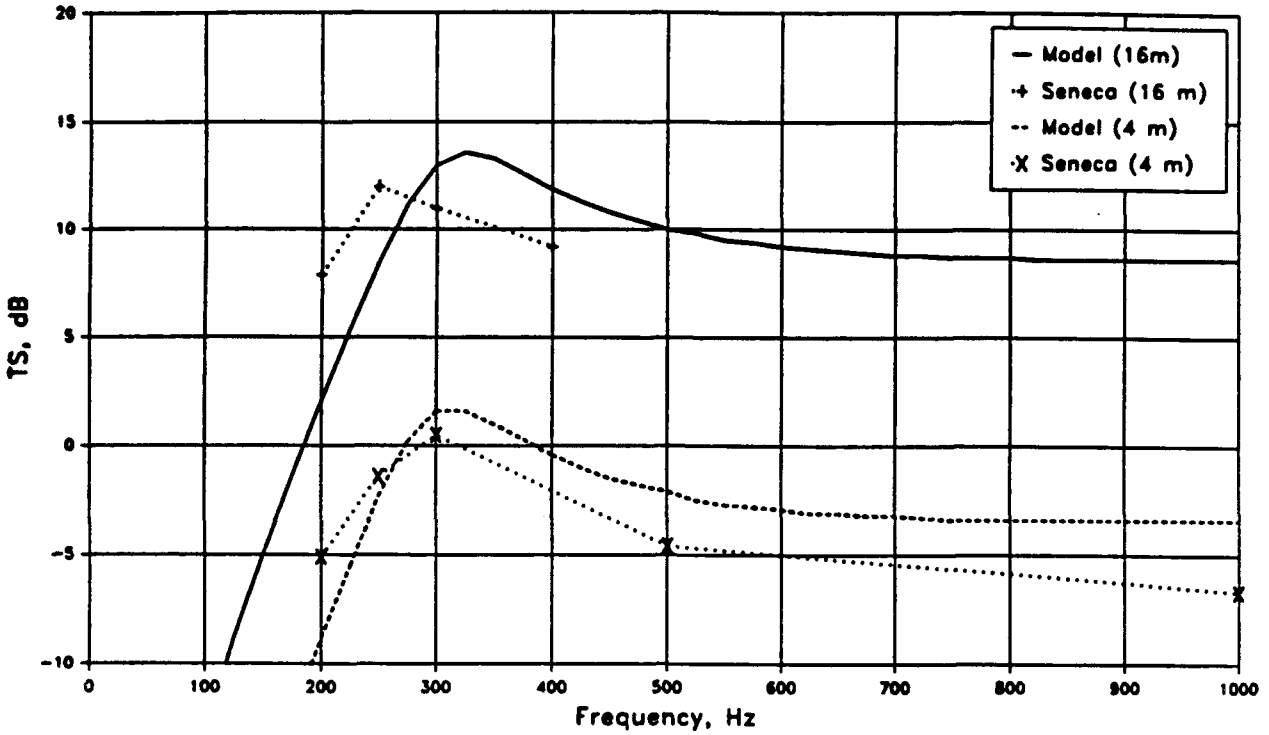

Figure 22. Predicted target strength compared with measured data, prototype reflector tubing tested at NUWC Lake Seneca Facility, depth 90 m (300 ft).

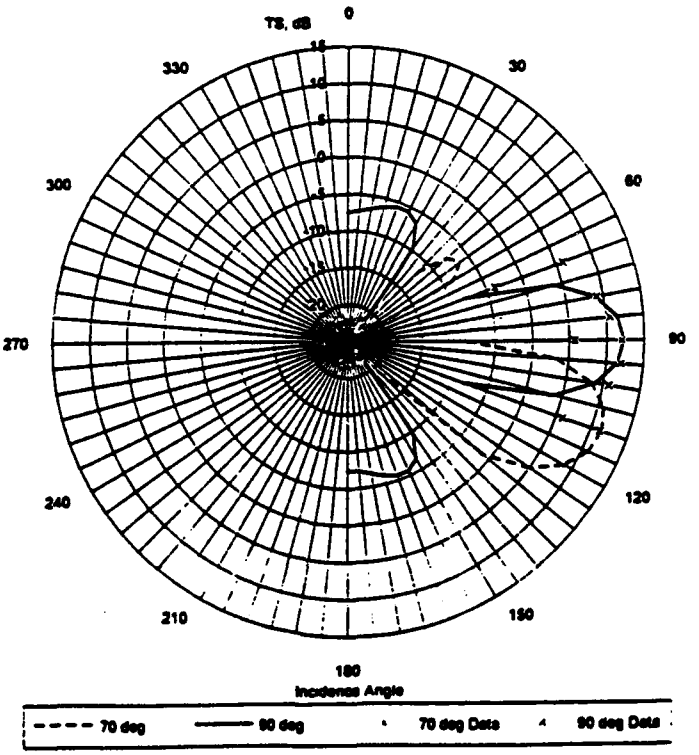

Figure 23. Bistatic vertical directionality, model prediction compared with measured data, length 16 m, frequency 250 Hz, depth 90 m (300 ft).

compare well with the predicted values but the measured beam pattern is broader than predicted. Fortunately this is a desirable result because it implies that the reflector is less sensitive to tilt effects than predicted. For oblique incidence, the directly backscattered sound is 15 dB down from the sound reflected at the specular angle (110°). Sound scattered horizontally is 6 dB down from the level observed at the specular reflection angle. Again, the measured beamwidth is wider than the predicted beam pattern.

5. FURTHER APPLICATIONS

The general design of the prototype reflector may be easily modified to change target strength values, vertical and horizontal directivity characteristics, and frequency response. The target strength can be increased by (a) increasing the length of the tube, (b) increasing the number of tubes, or (c) increasing the diameter of the tube(s).[7] Vertical directivity is changed when the length of the tube is changed (longer tubes produce higher target strength with narrower vertical beamwidth). Horizontal directivity is changed if several tubes are deployed in close proximity with a spacing $\leq \lambda/2$. As shown previously in Fig. 15, measurements in the test tank with 2 - 7.8 mm (5/16 in.) OD, 0.4 m (16 in.) long tubes gave TS increases up to 5 dB using a $\lambda/4$ spacing. These scale-model results show that target strengths up to 18 dB at 250 Hz could be obtained by deploying two prototype reflector units side-by-side with 1.5 m horizontal separation.

Appendix C contains a description of the design of a longer reflector (32 m) with performance down to 100 Hz. Following a number of design iterations, this broadband reflector was constructed for use in the ACT-II sea trials in August and September 1993.

Other means for horizontal and vertical directivity modification may employ simulation of a larger gas-filled cylinder by using a ring of gas-filled tubes having a diameter equal to the simulated cylinder. The spacing between the tubes should be at least $< \lambda/2$ and preferably $< \lambda/4$ for best results. The resonance frequency of each of these tubes must be comparable to or lower than the desired operating range.

[7]Increasing the tube diameter will increase target strength at high frequencies ($ka \geq 1.0$), but not at resonance.

6. REFERENCES

Anderson, V.C. 1950. "Sound scattering from a fluid sphere." *J Acoust. Soc. Am.* **22**:426-431.

Carey, W.M., J.W. Fitzgerald, and D.G. Browning./ 1990. "Low-frequency noise from breaking waves." NUSC Tech. Rep. 8783, DTIC No. AD227969.

Clay, C.S. 1991. "Low-resolution acoustic scattering models: Fluid-filled cylinders and fish with swim-bladders." *J. Acoust. Soc. Am.* **89**:2168-2178.

Stanton, T.K. 1988. "Sound scattering by cylinders of finite length. I. Fluid cylinders." *J. Acoust. Soc. Am.* **83**:55-63.

Stanton, T.K. 1989. "Simple approximate formulas for backscattering of sound by spherical and elongated objects." *J. Acoust. Soc. Am.* **86**:1499-1510.

Toulis, W.J. 1957. "Acoustic refraction and scattering with compliant elements, I. Measurements in water." *J. Acoust. Soc. Am.* **29**:1021-1026.

Weston, D.E. 1966. "Acoustic interaction effects in arrays of small spheres." *J. Acoust. Soc. Am.* **39**:316-322.

Urick, R.J. 1983. *Principles of Underwater Sound.* McGraw-Hill, Inc., New York, p.304.

Appendix A. Empirical equations for the backscattering target strength of finite cylinders

Stanton (1989) presented several empirical equations for the backscattering target strength of finite cylinders that were based on the frequency response functions of high-pass filters. The formulation specific for gas-filled cylinders was used as the basis for developing an equation that incorporates the effects of depth pressure on the target strength function. The frequency response curves and the depth versus target strength characteristic presented by Clay (1991) were used to determine depth-dependent coefficients for Stanton's equation based on an empirical fit to Clay's reported results. The reformulation of Stanton's equation was in the form

$$TS(ka,Z) = 10Log_{10}\frac{.25L^2(ka)^4S^2G}{\alpha^{-2}+\frac{\pi(ka)^3}{R^2F}} \qquad \text{(A1)}$$

where Z = Depth (m)
$\theta = \pi/2$, Incidence angle

$$g = .0012(1+0.1Z)^{-1} \qquad \text{(A2) (density ratio)}$$

$$h = 0.23(1+1.1\cdot10^{-5}Z)^{-1} \qquad \text{(A3) (sound speed ratio)}$$

$$S = \frac{\sin(kLcos\theta)}{kLcos\theta} \qquad \text{(A4)}$$

$$G = 1+C_3e^{-C_1(ka-C_2)^2} \qquad \text{(A5)}$$

$$C_1 = 9*10^5(1+0.1Z)^{1.21} \qquad \text{(A6) (bubble damping)}$$

$$C_2 = .0045(1+0.1Z)^{.367} \qquad \text{(A7) (bubble resonance)}$$

$$C_3 = 20(1+0.1Z)^{.28} \qquad \text{(A8) (amplitude coefficient)}$$

$$\alpha = \frac{1+gh^2}{2gh^2}+\frac{1-g}{1+g} \qquad \text{(A9)}$$

$$R=\frac{gh-1}{gh+1} \qquad \text{(A10) (reflection factor)}$$

$$F=1+0.35(ka)^{-0.8} \qquad \text{(A11)}$$

Figure A1 shows a comparison between results from the computer model based on Stanton's analysis and results from Eqn. (A1) for air-filled cylinders at depths of 10, 30, and 100 m. The results are normalized to a length of 1 m. Adjustments for other length cylinders may be made by adding the factor $20\text{Log}_{10}(L)$ to the value obtained from Fig. A1 for a given value of ka and depth.

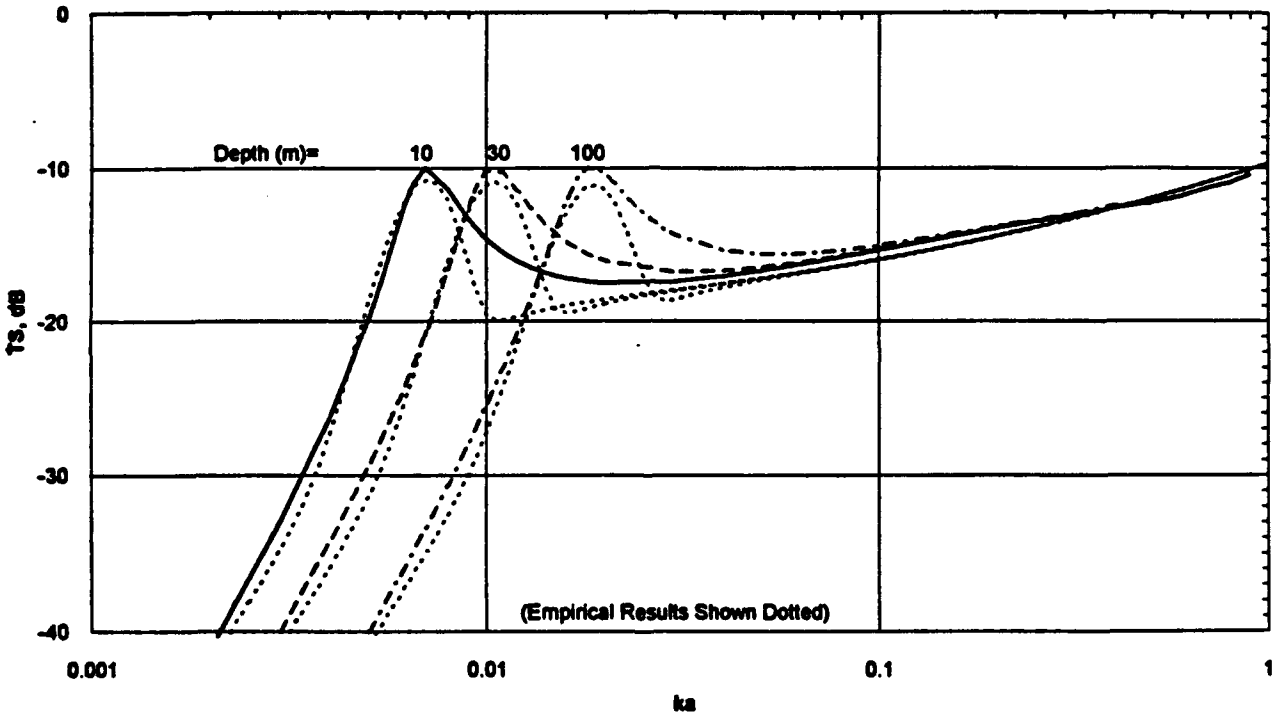

Figure A1. Target Strength for Air-Filled Cylinders, Analytic Model and Empirical Equation Results for L = 1 m.

APPENDIX B.

To: C. I. Malme, J. C. Heine

From: P. W. Jameson, D. Zwillinger

Subject: Converting Near-Field Measurements to Target Strengths

Date: December 14, 1992

1 Target Strength Measurements

Target strength is defined in terms of a situation in which the target is in the far-field of both the source and the receiver. The target is insonified by a wave which is approximately plane and the received signal is expressed in terms of a source centered on the target and spreading spherically. Target strength is defined as ten times the logarithm of the square of the ratio of the scattered pressure at a meter from the center to the incident plane wave pressure.

In experiments in the BBN tank and at Lake Seneca, both the source and the receiver were at distances from a target cylinder comparable to that of the length of the cylinder, and the assumptions of the target being in the far-field were not met. To determine the relationship between a measurement of the target strength of an object in the far-field of both the source and receiver and the recent measurements in the BBN tank and Lake Seneca we will evaluate a model of an experiment at similar ranges and make a direct comparison. We will use computed results to make precise comparisons between far-field target strength and near-field apparent target strength.

1.1 Mathematical Analysis

Consider the geometry shown in figure 1. Note that the radius of the cylinder is a.

Define $\mathrm{u}(\mathrm{r},t)$, $\mathrm{v}(\mathrm{r},t)$ and $p(\mathrm{r},t)$ to be the displacement, velocity, and pressure at any point r; each of these contains the time harmonic factor $e^{-i\omega t}$ (i.e., the pressure function has the form $p(\mathrm{r},t) = P(\mathrm{r},\omega)e^{-i\omega t}$). Let $u_r(a,z,t)$ and $U_r(a,z,\omega)$ denote the radial displacement on the surface of the cylinder. Similarly, $v_r(a,z,t)$ and $V_r(a,z,\omega)$ will denote the radial velocity on the surface of the cylinder.

We make the following assumptions:

- The effect of translational motion can be neglected (i.e., there is no substantial effect from "rigid body" motion of the cylinder)
- The surface of the cylinder is a pressure release surface, so that the pressure is zero on the surface of the cylinder: $p(r=a,z,t)=0$
- The radial velocity at the surface of the cylinder is proportional to the local pressure field incident on the cylinder. This is more likely to be true for low frequencies. We assume that the constant of proportionality relating displacement and incident pressure is C^{-1} so that $U_r(z,\omega) = P_i(r=0,z,\omega)/C$.

We note that Green's second theorem[1] states

$$P_\omega(\mathrm{r}) = \int_{S_0}\int \left[G_\omega(\mathrm{r}|\mathrm{r}_0)\frac{\partial P}{\partial r} - P(\mathrm{r}_0)\frac{\partial G_\omega(\mathrm{r}|\mathrm{r}_0)}{\partial r}\right] dS_0 \qquad (1)$$

[1] See D. Zwillinger, *Handbook of Integration*, Jones & Bartlett, Inc., 1992 and P. M. Morse and K. U. Ingard, *Theoretical Acoustics*, McGraw-Hill, 1968, page 321, equation (7.1.17).

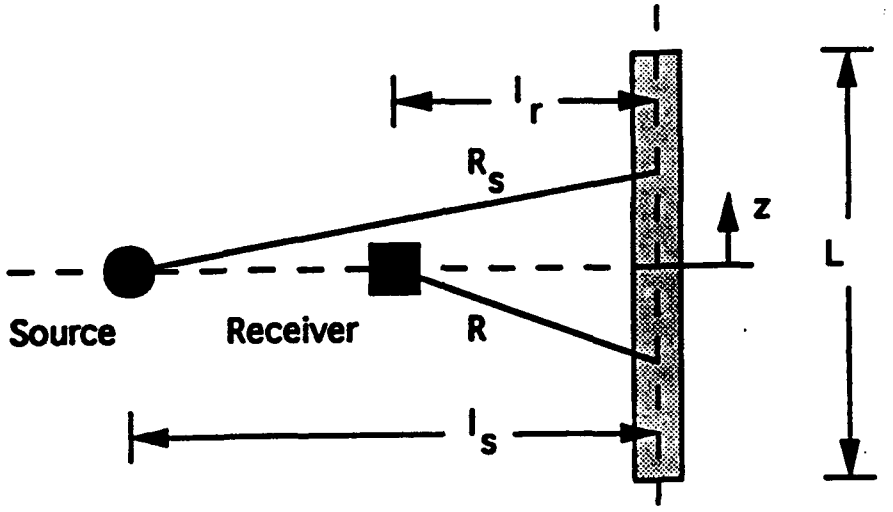

Figure 1: Arrangement of source, receiver, and target.

where $G_\omega(\mathbf{r}|\mathbf{r}_0)$ denotes the Green's function for a source at $\mathbf{r}_0$ which is received at $\mathbf{r}$, and the integration region S_0 is the surface of the cylinder. We will use the free-space Green's function for our problem so that $G_\omega(\mathbf{r}|\mathbf{r}_0) = e^{ikR}/4\pi R$, where $R = \sqrt{|\mathbf{r}|^2 - |\mathbf{r}_0|^2} \approx \sqrt{l_r^2 + z^2}$.

From the Navier-Stokes equation[2] we have

$$\rho \frac{\partial v_r}{\partial t} = -\frac{\partial p(\mathbf{r},t)}{\partial r}$$

Using our above approximations, and the definition $v_r = \partial u_r/\partial t$, this becomes

$$\left.\frac{\partial P}{\partial r}\right|_{r=a} = \rho\omega^2 U_r \tag{2}$$

Using (2) in (1) results in (note that the second term in 1 vanishes identically because $P(\mathbf{r}_0)$ is assumed to vanish on the surface of the cylinder)

$$P_\omega(\mathbf{r}) = \int_{-L/2}^{L/2} dz \int_0^{2\pi} a\, d\theta \frac{e^{ikR}}{4\pi R} \frac{\rho\omega^2 P_i(z)}{C}$$

If we use a spherically spreading wave for the incident field, then we have $P_i(z) = P_s \ell_{ref} e^{ikR_s}/R_s$ where $R_s = \sqrt{|\mathbf{r}_s|^2 - |\mathbf{r}_0|^2} \approx \sqrt{l_s^2 + z^2}$ and ℓ_{ref} is a standard reference range. This results in an expression for the scattered field at the receiver position

$$P_\omega(\mathbf{r}) \approx \frac{P_s \ell_{ref} \rho\omega^2 a}{2C} \int_{-L/2}^{L/2} dz \frac{e^{ik\left[\sqrt{l_r^2+z^2}+\sqrt{l_s^2+z^2}\right]}}{\sqrt{l_r^2+z^2}\sqrt{l_s^2+z^2}}$$

The apparent target strength, $\widehat{\mathrm{TS}}$, is defined in terms of the reference range ℓ_{ref} by

$$\widehat{\mathrm{TS}} = 10\log\left|\frac{P_\omega(\mathbf{r})\left.\frac{R}{\ell_{ref}}\right|_{ave}}{P_s\left.\frac{\ell_{ref}}{R_s}\right|_{ave}}\right|^2 = 10\log\left|\frac{P_\omega(\mathbf{r})\,(l_r/\ell_{ref})}{P_s\,(\ell_{ref}/l_s)}\right|^2$$

[2] See D. Zwillinger, *Handbook of Differential Equations*, Academic Press, 1992.

(The notation $R\big|_{z=0}$ indicates the distance from the source to the axis of the cylinder, when $z = 0$.) For the far-field case we have $l_r \gg 1$ and $l_s \gg 1$. In this limit we find

$$\frac{P_\omega(\mathbf{r})\dfrac{R\big|_{z=0}}{l_{ref}}}{P_s\dfrac{l_{ref}}{R_s\big|_{s=0}}} \longmapsto \frac{\rho\omega^2 a}{2C}e^{ik(l_r+l_s)}\frac{L}{l_{ref}}$$

so that the far-field target strength is

$\mathrm{TS} = 10\log\left|\frac{\rho\omega^2 aL}{2Cl_{ref}}\right|^2$. Since we are interested in how this differs from the apparent target strength, we compute the ratio

$$\text{apparent TS} - \text{far-field TS} = 10\log\left|\frac{l_r l_s}{L}\int_{-L/2}^{L/2} dz\,\frac{e^{ik\left[\sqrt{l_r^2+z^2}-l_r+\sqrt{l_s^2+z^2}-l_s\right]}}{\sqrt{l_r^2+z^2}\sqrt{l_s^2+z^2}}\right|^2. \qquad (3)$$

This function was evaluated numerically for two specific sets of parameters.

1.2 Numerical Studies

The integral in (3) was evaluated for two different cases: a short reflector and a long reflector. These two cases are defined as follows

- Short reflector: $L = 4.9$ m, $l_s = 16.2$ m, $l_r = 23.9$ m
- Long reflector: $L = 17$ m, $l_s = 42.7$ m, $l_r = 33.2$ m

For these two cases, we find the following relationship between apparent target strength and far-field target strength at certain selected frequencies

- Short reflector:

  3 kHz: −4.1 dB

- Long reflector:

  200 Hz: −1.3 dB
  250 Hz: −1.9 dB
  300 Hz: −2.7 dB
  400 Hz: −4.8 dB

1.3 Extensions of this work

There are some natural extensions that can be performed on this work. For example, we could consider angle effects and investigate the effect of higher order modes of the reflecting cylinder.

2 Notation

a	radius of cylinder
c	acoustic soundspeed
C	constant of proportionality
L	length of cylinder
l_r	distance from center of cylinder to the receiver

l_s	distance from center of cylinder to the source
m	azimuthal mode number
m	"meters"
ω	frequency
p	pressure
P_i	incident pressure
P_ω	pressure due to the scattered wave
ρ	density
t	time
TS	target strength
$\widehat{\text{TS}}$	apparent target strength
u	displacement
u_r	radial displacement
v	velocity
v_r	radial velocity

APPENDIX C: SUMMARY OF BROAD-BAND REFLECTOR DESIGN, JUNE-JULY 1993

This appendix documents the design of a broad-band reflector for use in both the ACT-II Gulf Tests and ACT-II Hudson Canyon Tests, which occurred in August and September of 1993, respectively. It is based on a "Memo to File" written by Paul McElroy on 9 July 1993, with a limited set of subsequent modifications and updates.

ACT-II Sea-Test Requirements. The ACT-II experiments occurred in Hudson Canyon in September 1993, and required a reflector for source monitoring, and as a reference target. Previous to these tests, the ACT-II Gulf Tests took place in the Gulf of Mexico, for the purpose of evaluating new source designs and assessing the reflector performance. For both tests, BBN participants wanted a passive reflector that was effective to lower frequencies than the original "narrow-band" unit, which has been documented extensively in the main body of this report. The lower frequency bound was to be 100 Hz, and the upper was to extend as high as possible (up to 500, or even 800 Hz).

Development of general design procedures for a broadband reflector of this type was initially proposed under P93-S&S-C-015 in response to DARPA BAA 93-04. However, rapid development of a prototype broadband unit was authorized under the UNDOA contract to serve as the target for the ACT-II tests. We note that the design could not be optimized under these time and financial constraints, but was to attain as many of the performance goals as practicable. In particular, it was not possible to carry out the major re-design necessary to ensure ease in deployment and recovery; that was to be a key feature of the new work in our proposal. In the event, deployment and recovery of the two passive reflectors used in the Hudson Canyon tests was fraught with difficulties, which provide a strong incentive for the major re-design envisioned in the proposal.

Goals in Designing a Broadband Reflector: Design of a multi-tube rubber-tube reflector suitable for use over a broad bandwidth of 100 to 500 Hz; performance to 800 Hz, broadside to this reflector, is desired if possible. The broadside performance shall be flat within ±1 dB, about a nominal Target Strength of 15 dB. The backscattered beam pattern shall have a half-beamwidth of at least 13 degrees (6 dB down point) starting at 100 Hz; this beamwidth performance is desired as high in frequency as possible. (The beam patterns studied analytically are two-way patterns, caused by the superposition of incoming and back-scattered energy at a given angle off broadside; however, one-way patterns can be inferred from the same plots.)

In selecting a design, we have set the following priorities amongst the several goals:

1 *Mean broadside TS of 15 dB.* This implies the lowest-frequency tube must be at least 16 meters in length. All initial designs have been based on this length (see Item 4.).

2 *TS flat within ±1 dB* over the range of 100-800 Hz. All designs examined which met this criterion were retained for further consideration in meeting the beamwidth criterion (Item 3).

3 Two-way 6-dB *full beamwidths of 26 degrees* (half beamwidths of 13 degrees) were sought over as large a frequency range as possible, starting at 100 Hz.

4 *Improved beamwidths at the cost of Broadside TS.* Once an acceptable design was achieved, changes in performance were assessed when this length was reduced to 12m and 8m; beam widths were improved at the cost of decreases in the low-frequency level.

Analytical Procedures. The Program ARMAC was used to predict tube response. Some approximations were necessary, such as the assumption that tube response off-normal is well represented by the response for normal incidence; this is equivalent to a point-reacting representation. Despite this approximation, the geometry (i.e., phase relationships) of off-normal incidence and scattering were properly represented.

The responses of individual tubes were then added coherently to give the composite response of the overall linear array. Interaction effects between tubes were not modeled.

Features of the tubes which were modeled were depth (internal pressure); inner diameter, wall thickness, and length; and elastomer properties (modulus and loss factor).

Number of Tube Diameters. Reflector designs can contain one or many different tubing diameters. The starting point in our design process was a three-tube-diameter design. However, those designs satisfying the first two goals showed poor beamwidths commencing at 150 Hz due to a deep hollow. The use of a four-tube-diameter design filled in the hollow, giving far better beamwidth performance.

Aneurysms. It was observed experimentally by our engineers during tests that 3-inch-ID tube sections more than 4 meters in length were subject to aneurysms. This restricts individual tube length to four meters and is consistent with our use of four tubes (constructed in 4-meter sections). (Note that in future work, the use of reinforced tubing may make this restriction to four-meter lengths unnecessary.)

Components of Candidate Design. The components are as follows:

1 Four tubing inner diameters: 3.00", 2.00", 1.50", and 1.25".

2 Four meter standard length

The different tubing diameters have the following total length and number of standard lengths:

Diameter	Total Length	Number of 4-meter sections
3.00	16m	4 x 4m
2.00	8m	2 x 4m
1.50	4m	1 x 4m
1.25	4m	1 x 4m

If the individual 4-meter sections are constructed as independent modules, they can be interconnected in a number of different ways, offering different tradeoffs of the three initial goals listed above.

Candidate Designs. There are at least two arrangements of the components listed above as shown in Fig. C-1.

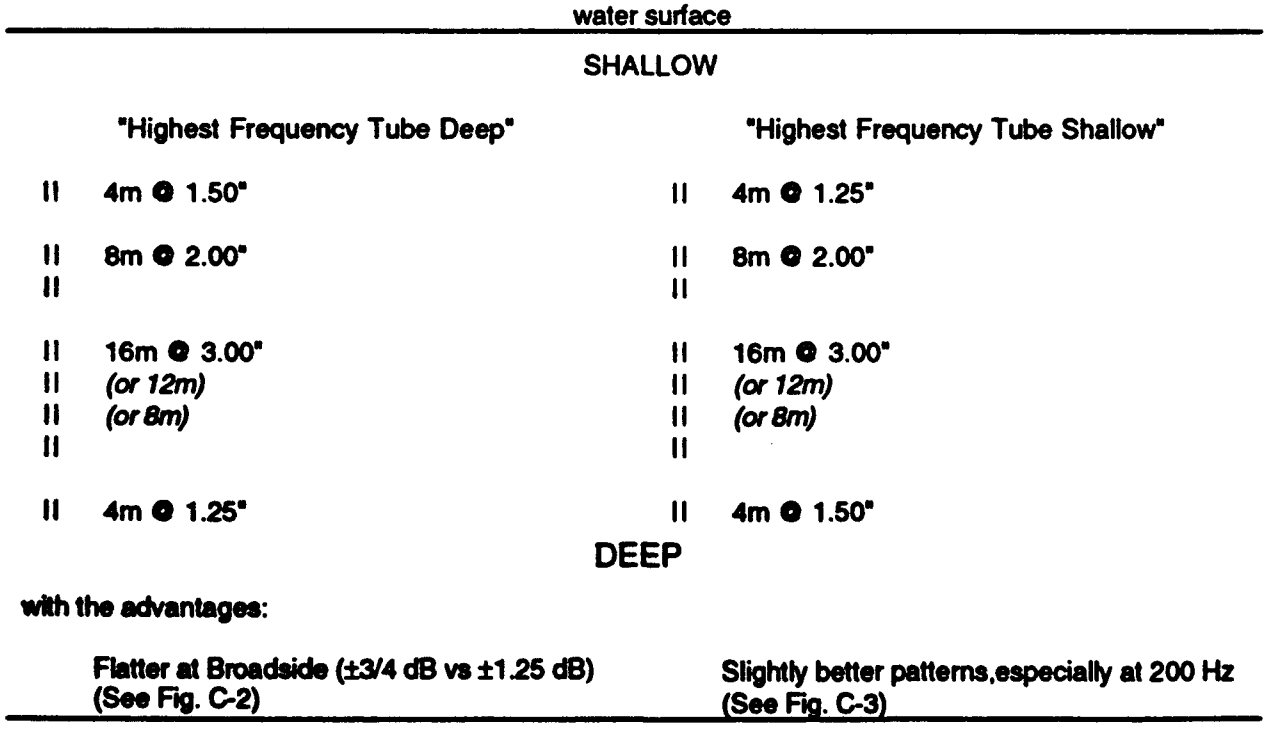

Figure C-1. Candidate arrangements of four tubing diameters for use in a Broadband Passive Reflector.

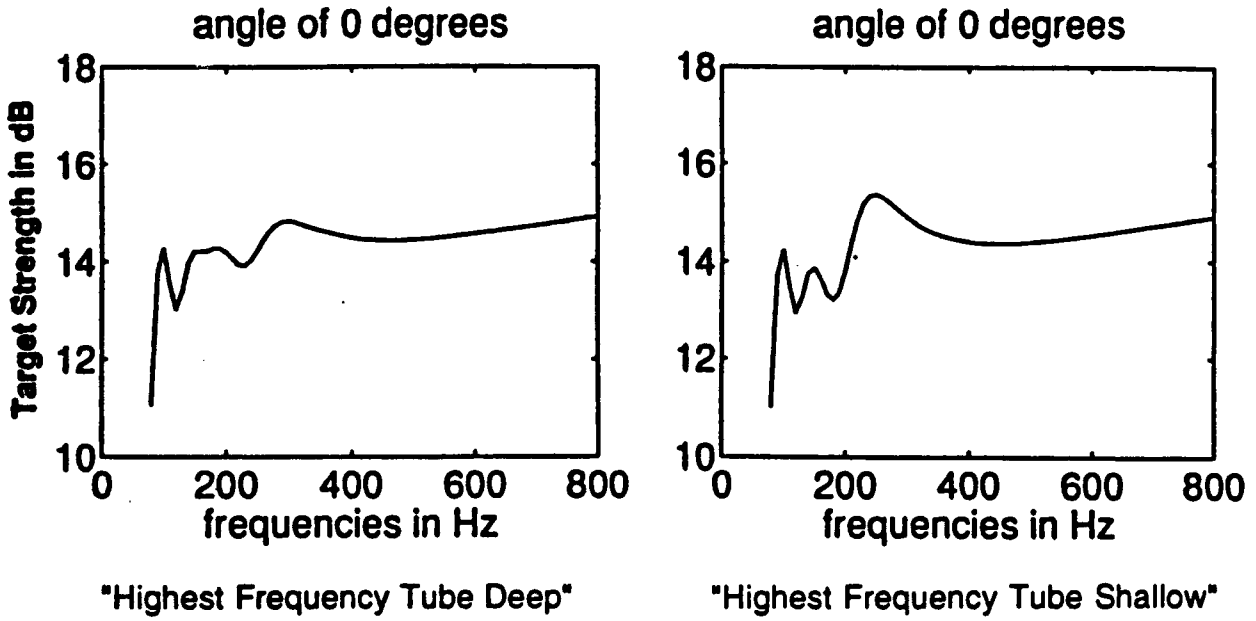

Figure C-2. Slight Sensitivity of Broadside Performance in Broadband Reflector to Arrangement of the High-Frequency Tubes.

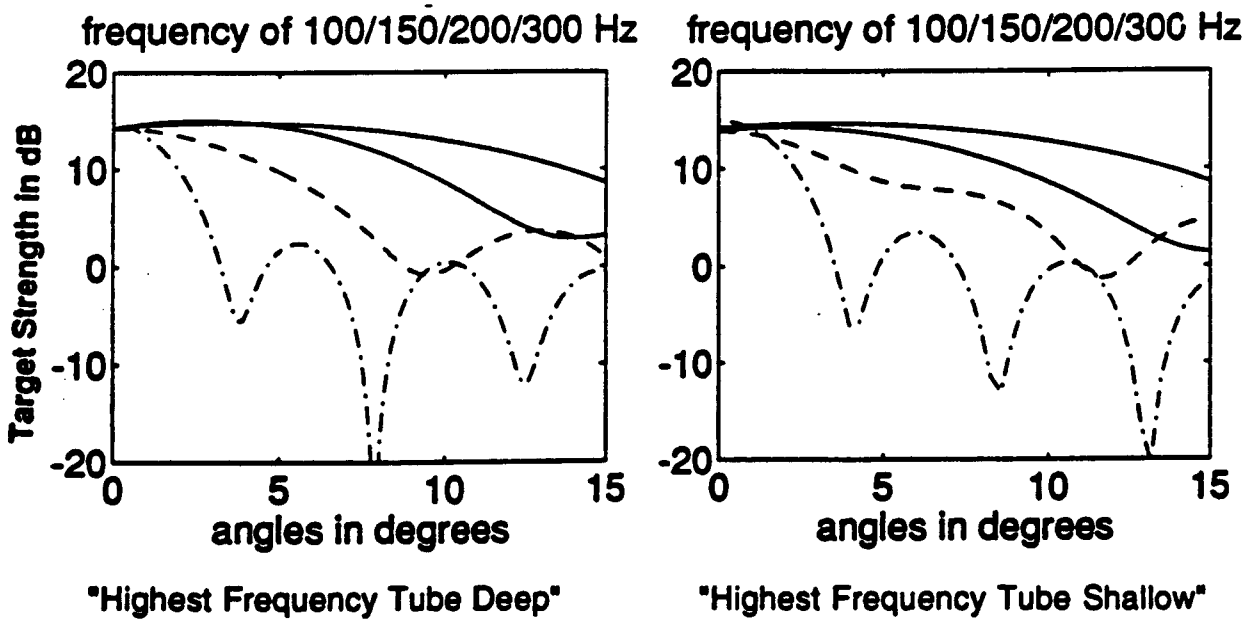

Figure C-3. Beam-Pattern Dependence at four frequencies upon the Arrangement of the High-Frequency Tubes (near-flat solid - 100 Hz; curved solid - 150 Hz; dashed - 200 Hz; dash-dot - 300 Hz)

In addition to the two primary arrangements shown in Fig. C-1, which comprise a full 32-meter reflector, there are numerous subsidiary arrangements *(noted in italics in the figure)* which involve the elimination of one or two 4-meter sections of the 3.00 in. tube. Whatever number of 3.00 in. tube sections are used, they should be contiguous, and in the center of the array; if separated, the sections partially cancel one another, reducing beamwidth at low frequencies.

Note that the use of 4-meter modules permits considerable mixing and matching of the tubes to attain different performance goals.

Why shorten the 3.0 inch section? Shortening the three-inch section to 12 or even 8 meters progressively improves the beam patterns at 100, 150, and 200 Hz, with loss of flatness at broadside. The drop at 100 Hz is 2.5 dB with the 12m and ~4 dB with the 8m (Fig. C-4). There are no significant improvements in beam pattern at 300 Hz and above through use of the shorter 3.00 inch segments.

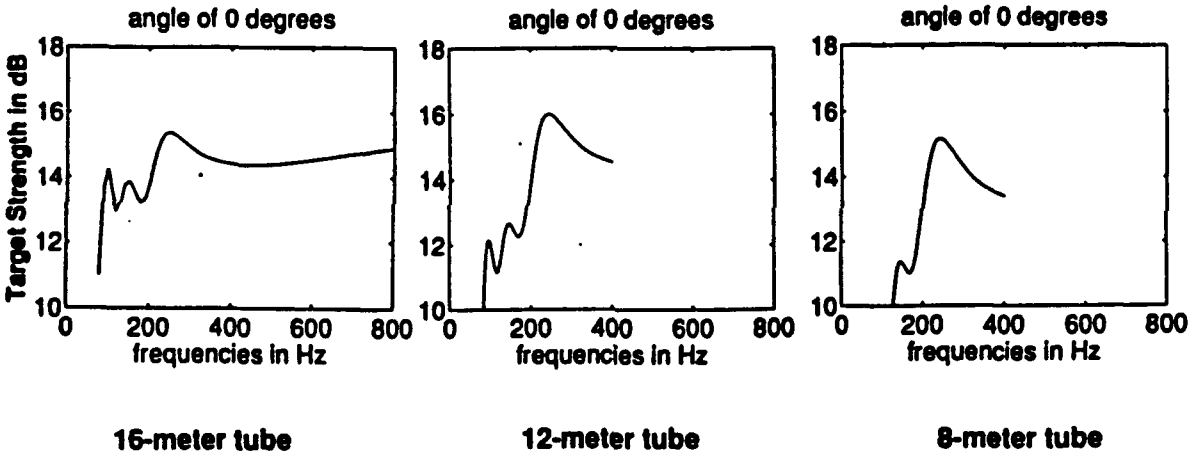

Fig. C-4. Variation in Broadside Performance when Shortening the Lowest-Frequency Tube.

Selected Design. The BBN staff utilizing the reflector in the ACT-II experiments selected the full 32-meter design shown on the right in Fig. C-1, since they preferred the better beam patterns to maximum flatness at broadside. This choice was made after a review of numerous plots of predicted performance, such as shown in Figs. C-2 through C-5. Figure C-5 is a color contour of the beam pattern for the full 32-meter reflector, which was selected for use in ACT-II. Figures C-2 through C-4 are two-dimensional cuts taken from these three-dimensional beam patterns.

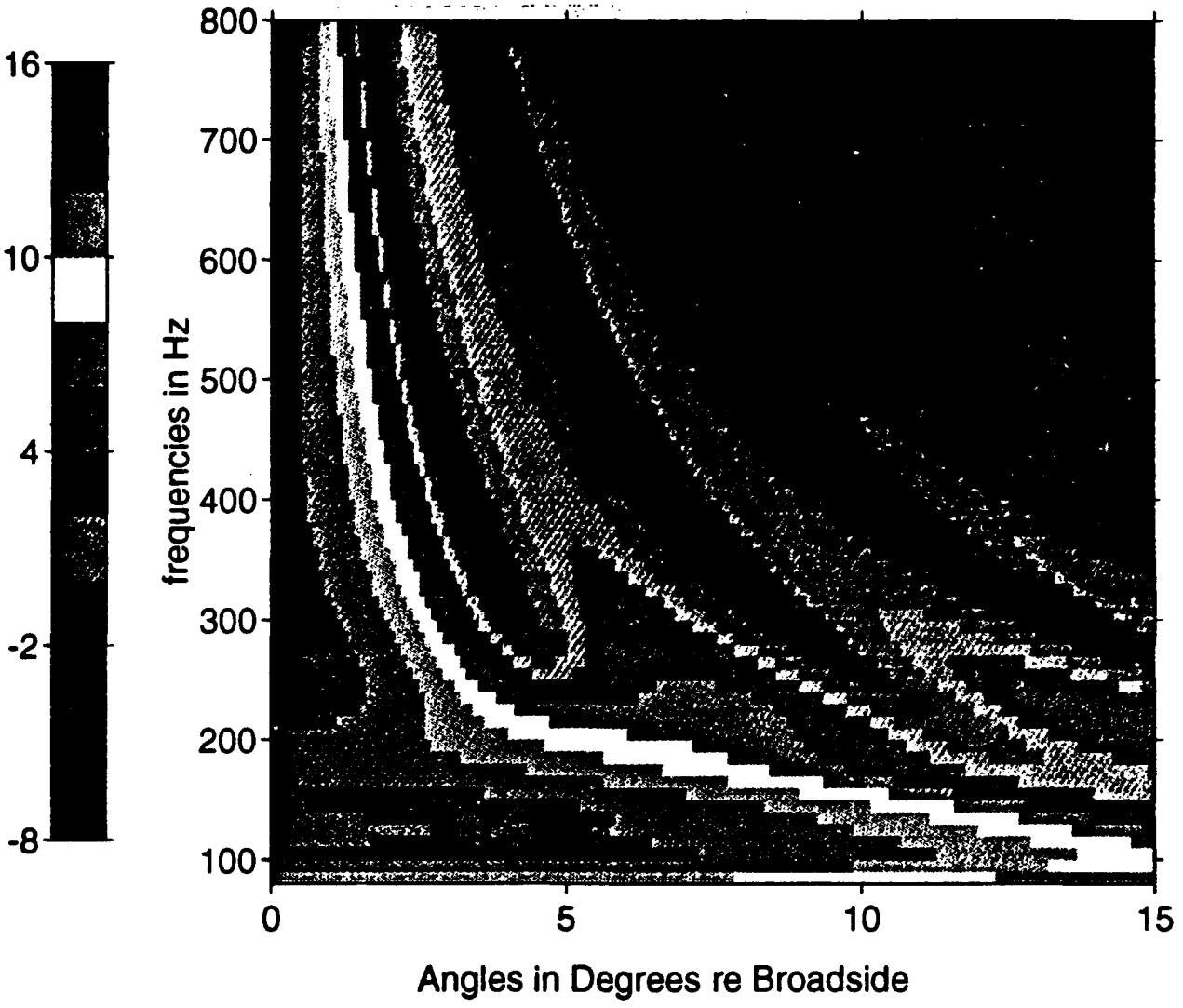

Figure C-5. Beam pattern versus frequency of 32 meter broadband reflector, composed of four different diameter tubes.

Future Issues. The following issues were not been resolved in the limited design process employed here:

1. What happens with an interchange of the 2.00 in. and 3.00 in. sections? Differences will arise from their depth dependences.

2. Is there an improvement with a 1.00 in. tube in place of the 1.25 in. tube?

3. Determine robustness of the solution with changes such as

   a. stiffer rubber, simulating the increase of the dynamic modulus over the static in elastomers,

   b. angular misalignments of the sections.

More generally, we will want to look at the effect of many segments, all 4 meters long and of different diameters, in the future. Development of more robust design guidelines would also be useful.

A ruggedized version of the passive reflector is necessary and would be easier to deploy and recover; deployment issues would be central in developing such an enhanced design.

DISTRIBUTION

BBN Report 7943, "Development of a High Target Strength Passive Acoustic Reflector of Low-Frequency Sonar Applications," by Charles Malme, et al.

Distribution Required by the Contract

Advanced Research Projects Agency (ARPA/ASW - Dr. W. Carey, Dr. T. Kooij) (2 copies)

Advanced Research Projects Agency (ARPA/UWO - Captain E. Mihalek)

Advanced Research Projects Agency - Contract Management Office (ARPA/CMO - Mr. G.E. Mayberry)

Defense Technical Information Center (DTIC) (2 copies)

Additional Distribution Recommended by ARPA

BBN Systems and Technologies (Dr. P. Cable, M. Steele)

Johns Hopkins University/ Applied Physics Laboratory (JHU/APL - G.R. Thompson, E.R. Bohn)

Naval Air Systems Command (NAVAIR PMA-264)

Naval Sea Systems Command (NAVSEA PMO-183)

Office of Naval Research (ONR-B. Blumenthal)

Chief of Naval Operations (OPN874N)

Chief of Naval Operations (OPN875)

ORINCON Corporation - Arlington (Dr. H. Cox)

Science Applications International Corportation - New London (SAIC - Dr. R. Evans)

Science Applications International Corportation - San Diego (SAIC - Dr. R. Himbarger)

Space and Naval Warfare Systems Command (SPAWAR - PD80, PMW182, PMW184)